Journal of proteome research

pubs.acs.org/jpr

Article

Cellular Imprinting Proteomics Assay: A Novel Method for Detection of Neural and Ocular Disorders Applied to Congenital Zika Virus Syndrome

Livia Rosa-Fernandes,*,◆ Raquel Hora Barbosa,◆ Maria Luiza B. dos Santos, Claudia B. Angeli, Thiago P. Silva, Rossana C. N. Melo, Gilberto Santos de Oliveira, Bernardo Lemos, Jennifer E Van Eyk, Martin R. Larsen, Claudete Araújo Cardoso, and Giuseppe Palmisano*

Cite This: *J. Proteome Res.* 2020, 19, 4496–4515

Read Online

ACCESS | Metrics & More | Article Recommendations | Supporting Information

ABSTRACT: Congenital Zika syndrome was first described due to increased incidence of congenital abnormalities associated with Zika virus (ZIKV) infection. Since the eye develops as part of the embryo central nervous system (CNS) structure, it becomes a specialized compartment able to display symptoms of neurodegenerative diseases and has been proposed as a noninvasive approach to the early diagnosis of neurological diseases. Ocular lesions result from defects that occurred during embryogenesis and can become apparent in newborns exposed to ZIKV. Furthermore, the absence of microcephaly cannot exclude the occurrence of ocular lesions and other CNS manifestations. Considering the need for surveillance of newborns and infants with possible congenital exposure, we developed a method termed cellular imprinting proteomic assay (CImPA) to evaluate the ocular surface proteome specific to infants exposed to ZIKV during gestation compared to nonexposure. CImPA combines surface cells and fluid capture using membrane disks and a large-scale quantitative proteomics approach, which allowed the first-time report of molecular alterations such as neutrophil degranulation, cell death signaling, ocular and neurological pathways, which are associated with ZIKV infection with and without the development of congenital Zika syndrome, CZS. Particularly, infants exposed to ZIKV during gestation and without early clinical symptoms could be detected using the CImPA method. Lastly, this methodology has broad applicability as it could be translated in the study of several neurological diseases to identify novel diagnostic biomarkers. Data are available via ProteomeXchange with identifier PXD014038.

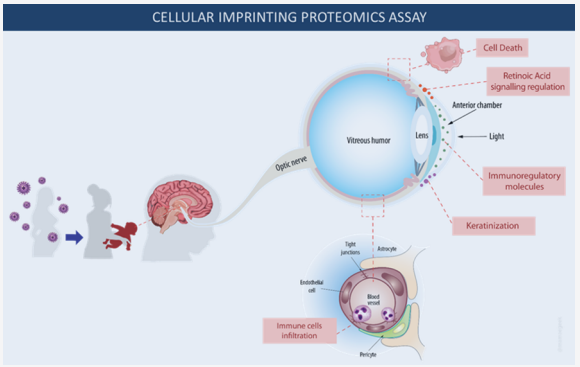

KEYWORDS: *impression cytology, Zika virus, ocular disorders, neutrophil degranulation, cellular imprinting proteomic assay, mass spectrometry*

INTRODUCTION

Zika virus (ZIKV) is a positive-strand RNA virus belonging to the *Flaviviridae* family transmitted to humans predominantly by the female *Aedes aegypti* and *Aedes albopictus* mosquitos.[1] Long after the first report of ZIKV infection in a nonhuman primate was made in 1947,[2] the first human infection was reported in Nigeria[3] with subsequently outbreaks in Micronesia and French Polynesia.[4] In 2015, clinicians in northeast Brazil correlated ZIKV infection with reports of newborns with microcephaly, congenital malformations, and neurological syndromes.[5] Since then, ZIKV infection raised global public health concerns due to its transmission potential and the fetal and neonatal abnormalities designated congenital Zika syndrome (CZS).[5] The syndrome characteristics include microcephaly, intracranial calcifications, spinal cord and peripheral nerve lesions, hemorrhage, and ocular pathology.[6,7] Indeed, several case reports and studies have described ocular pathologies in neonates born to mother infected with ZIKV during pregnancy.[8−14] However, microcephaly at birth is not the definitive hallmark of CZS.[15] Children born with normal head circumferences can still develop brain and other abnormalities as the prognosis for infants with congenital infection is not yet known.[15,16] The appropriate timing and assay for detection of congenital Zika virus infection are not yet defined,[16] which might compromise the identification of children without noticeable clinical findings at birth but who might develop

Special Issue: Proteomics in Pandemic Disease

Received: May 12, 2020
Published: July 19, 2020

later Zika-related complications, increasing the need for accurate early diagnostic approaches.

Even though the eye appears as a peripheral structure in the fully formed adult nervous system, the embryonic diencephalon gives rise to the optic nerve and retina in the developing brain. Consequently, the eye develops as an immune privileged site that shares a pattern of molecules and cytokines with the brain and spinal cord[17] potentially providing an noninvasive assessment of the CNS status. In fact, several brain pathologies have associated ocular abnormalities which have been described in patients with stroke,[18] multiple sclerosis,[19] Parkinson's,[20] and Alzheimer's diseases.[21] Notably, a common pattern of vision-threatening findings has been associated with congenital ZIKV infection and include chorioretinal atrophy, focal pigmentary changes in the macular region, and optic nerve abnormalities.[22] Anterior segment alterations have also been reported, such as iris coloboma and microphthalmia.[23] Moreover, ZIKV antigens were found in the iris, neural retina, choroid, and optic nerve in infants with CZS.[24,25]

The association of eye abnormalities with congenital ZIKV infection has been reported in infants with microcephaly, but, importantly, this also occurs in infants without CZS signs.[26−28] As the absence of microcephaly cannot exclude other CNS manifestations,[29] understanding the molecular profile underlining ocular abnormalities in ZIKV-infected infants is essential for a diagnostic and potentially therapeutic solution. Here we report the development of the cellular imprinting proteomic assay (CImPA) based on a combined ocular cell surface capture using membrane disks and a large-scale quantitative proteomics approach, which allowed us to map quantitatively the ocular cell surface proteome. Following its application in infants with intrauterine Zika virus infection, with and without microcephaly at birth, the CImPA method enabled the identification of a protein pattern that could discriminate ocular dysfunctions in infants exposed to ZIKV during gestation with diagnosed CZS at birth from the ones without early clinical findings.

SUBJECTS AND MATERIALS AND METHODS

Patient Cohort

This study comprises 13 infants with and without CZS referred to the Pediatric Service of the Antonio Pedro University Hospital, Fluminense Federal University, Niteroi, Brazil. This study was approved by Institutional Review Board and Ethics Committee of Fluminense Federal University, protocol CAAE number 79890517.6.0000.5243, and followed the guidelines of the Declaration of Helsinki. All samples were collected upon informed and written consent from the parents/legal guardians of each participant. Clinical examination was performed by a multidisciplinary team, and all infants included in this study are part of a clinical follow up program currently in progress.[30] CZS clinical diagnosis was based on the Brazilian Ministry of Health guidelines. Retrieved information is assembled in Tables 1 and 2 and Table S1.

Cellular Imprinting Proteomics Assay

Ocular Cells Collection and Protein Extraction on Nitrocellulose Membrane. Ocular surface cells were obtained through optimized impression cytology procedure as previously described.[31] The cell capture area of the nitrocellulose membrane was immersed in a low-binding Eppendorf tube containing 200 μL of protein extraction solution consisting of 1% sodium deoxycholate (SDC), 1× PBS and 1× protease inhibitor cocktail (Sigma-Aldrich) and incubated for 20 min under agitation at room temperature. Subsequently, the nitrocellulose membrane immersed in the extraction solution was probe tip sonicated using for three cycles for 20 s and intervals of 10 s on ice. Membranes from left and right eyes were sampled and analyzed separately as reported in Table 1. For the control condition, 12 membranes were collected, with eight (one on left and one on right eye) from four infants and four (two on left and two on right eye) from one infant.

Table 1. Clinical and Demographic Data of the Patient Cohort[a]

	Ctrl	Zikv	Zikv^{CZS}
no. of patients	5	5	3
age at sample collection (months, mean ± SD)	21.4 ± 1.8	22.4 ± 3.5	22.3 ± 4.2
Gender			
M	3	3	2
F	2	2	1
Sampling for proteomic analysis (no. of membranes/subject)[b]			
1	0	1	0
2	4	2	2
3	0	1	0
4	1	0	1
6	0	1	0
total	12	14	8
ZIKV exposition			
Y	0	5	3
N	5	0	0
ZIKV symptoms (trimester)			
1°		1	2
2°		1	1
3°		3	0
ZIKV congenital syndrome clinical diagnostics			
Y	0	0	3
N	5	5	0
Microcephaly			
Y	0	0	3
N	5	5	0
Vision impairment			
Y	0	0	2
N	5	5	1
type			optic disc excavation and pallor; abnormal pigment deposition and macular atrophy

[a]Ctrl: children with normal development, without ZIKV exposure. Zikv: children infected by Zika virus during gestation and without congenital Zika syndrome. Zikv^{CZS}: children infected by Zika virus during gestation and with congenital Zika syndrome. [b]More information about membrane collection and patients is reported in Table S7.

Protein Reduction, Alkylation, and Trypsin Digestion. Proteins were reduced with 10 mM DTT for 30 min at 56 °C and alkylated with 40 mM IAA for 30 min at room temperature, in the dark. Proteins were quantified using the nanodrop method before porcine trypsin (Promega) was added to a 1:50 ratio. The digestion, which proceeded for 16 h at 37 °C, was blocked by adding 1% TFA final concentration before the SDC was removed from the solution by centrifugation at 10000g for 10 min. Tryptic peptides were desalted using R3 microcolumns before LC-MS/MS analysis.[32−34]

Liquid Chromatography Mass Spectrometry Analysis. The peptide samples were loaded on an in-house packed

https://dx.doi.org/10.1021/acs.jproteome.0c00320
J. Proteome Res. 2020, 19, 4496−4515

Table 2. Clinical and Demographic Data of the Patient Cohort and Respective Mothers[a]

	Ctrl	Zikv	Zikv^{CZS}
birth date (semester)			
1°/2016	2	4	1
2°/2016	3	1	2
Encephalic perimeter (cm, mean ± SD)	33.4 ± 2.6	33.6 ± 1.5	29.5 ± 0.8
Apgar score			
0−3	0	0	0
4−6	0	1	0
7−10	5	4	3
Age mother (years, mean ± SD)	29 ± 9.1	29 ± 6.5	33,6 ± 12
Exanthema			
Y	5	5	3
N	0	0	0
PCR Zika mother			
positive	0	5	3
negative	5	0	0

[a]Ctrl: children with normal development, without ZIKV exposure. Zikv: children infected by Zika virus during gestation and without congenital Zika syndrome. Zikv^{CZS}: children infected by Zika virus during gestation and with congenital Zika syndrome.

precolumn (4 cm × 100 μm inner diameter, 5 μm particles) using an Easy-nanoLC system (ThermoFisher) and separated by gradient from 3 to 28% solvent B in 100 min, 28−45% in 20 min, 45−95% B in 2 and 8 min at 95% B (A = 0.1% FA; B = 90% ACN, 0.1% FA) at a flow of 250 nL/min on analytical Reprosil-Pur C18-AQ column (20 cm × 75 μm inner diameter, 3 μm particles). The Easy-nanoLC system was connected online to Orbitrap Fusion LumosTribrid mass spectrometer (Thermo Fisher) operating in positive ion mode and using data-dependent acquisition. The full MS scans were acquired over a mass range of m/z 350−1600 with detection in the Orbitrap at 120 000 resolution with AGC target set to 3e6 and a maximum fill time of 100 ms. Following each MS scan, the 20 most abundant peptide ions above a threshold of 50 000 were selected in the quadrupole with an isolation window of 0.7 m/z and fragmented using HCD fragmentation (collision energy: 35). Fragment ions were acquired in the orbitrap at 30 000 fwhm resolution for an ion target of 50 000 and a maximum injection time of 50 ms, dynamic exclusion of 30 s and fixed first mass 110 m/z. All data were acquired with Xcalibur software v3.0.63 (Tune v2.0 1258).

Database Search and Statistical Analysis. Raw data were searched using the MaxQuant v1.6.2.10 (MQ) and Proteome Discoverer v2.3.0.523 (PD) computational platforms using Andromeda (MQ) and Sequest search engines, respectively. The parameters used for database search were human reviewed proteome database (20 400 entries, downloaded from Uniprot the 01/2019) with the common contaminants, trypsin as cleavage enzyme, two missed cleavages allowed, carbamidomethylation of cysteine as fixed modification, oxidation of methionine, and protein N-terminal acetylation as variable modifications. Protein identification was accepted with less than 1% FDR. For the Proteome Discoverer platform, the percolator, peptide, and protein validator nodes were used to calculate PSMs, peptides, and proteins FDR, respectively. FDR less than 1% was accepted. Protein grouping was performed using the strict parsimony principle. Label-free quantification was performed in the two platforms using the extracted ion chromatogram area of the precursor ions activating the matching between run feature. Protein quantification normalization and roll-up were performed using unique and razor peptides and excluding modified peptides. The intensity based absolute quantification feature (iBAQ) was activated in MaxQuant to calculate the relative protein abundance within samples. Differentially regulated proteins between the three conditions were selected using t test with a posthoc background-based adjusted p-value <0.05.[35] Statistical analyses, volcano, and PCA plots were performed in the Perseus and Proteome Discoverer software. The data obtained from Proteome Discoverer were used as primary data and complemented with the MaxQuant data to prioritize proteins and biological processes.

Bioinformatic Analysis. The total identified proteins were compared with the human plasma proteome database. Regulated proteins were matched against the human protein atlas database using eye-enriched and brain-enriched proteins (https://www.proteinatlas.org/). Moreover, the NEIBank was used to retrieve disease genes that affect vision and other disease genes with eye phenotypes (https://neibank.nei.nih.gov/cgi-bin/eyeDiseaseGenes.cgi). A total of 441 and 165 genes associated with eye diseases and other diseases were retrieved, respectively. The human plasma proteome was retrieved from the Human Plasma Peptide Atlas, which contains 3509 proteins (http://www.peptideatlas.org/hupo/hppp/). Gene ontologies categories were retrieved using the Protein annotation node built-in Proteome Discoverer. Moreover, STRING database (https://string-db.org/) was used to build protein−protein interaction networks from regulated proteins and identify enriched Reactome and KEGG pathways at FDR < 0.05.

Protein Abundance Validation Using Parallel Reaction Monitoring (PRM)

Differentially regulated proteins were selected for further validation by parallel reaction monitoring using the following criteria: (a) protein differentially regulated with adjusted p-value < 0.05, (b) with more than or equal to two peptides, (c) with more than or equal to 1 unique peptide, (d) concordant abundance ratio of the peptides without missing cleavage, and (e) more than or equal to two unique peptides without missing cleavages found in more than 50% samples of each condition. Parallel reaction monitoring was performed using the same nLC-MS/MS setup described for the discovery experiment including a targeted mass list of peptides selected based on the characteristics described above. A list of peptides, m/z and z is provided (Table S2). The raw data were searched using Proteome Discoverer (Thermo) as described above for the

https://dx.doi.org/10.1021/acs.jproteome.0c00320
J. Proteome Res. 2020, 19, 4496−4515

samples acquired in data dependent mode. The peptide abundances were retrieved from the extracted ion chromatogram (XIC) and normalized by the total base peak intensity for each sample. Two tails *t* test statistic was performed to calculate differentially regulated peptides (p-value < 0.05) between the three conditions. ROC curves and the associated statistical parameters (cutoff, sensitivity, and specificity) were calculated using Metaboanalyst computational platform (https://www.metaboanalyst.ca) within the biomarker analysis pipeline. The multivariate ROC analysis was performed using Random Forest as classification and ranking method. AUC more than 0.8 on the two peptides belonging to each protein was considered as potential discriminative features.

Morphological Analysis and Image Acquisition

To evaluate microscopic features of the cells, the nitrocellulose membranes containing collected cells were fixed in 4% paraformaldehyde in phosphate buffer, pH 7.4 for 4 h, at room temperature, rapidly vortexed to allow release of adhered cells, and cytocentrifuged (Cytospin 4 Shandon, Thermo Scientific, Waltham, MA) at 1200 rpm, for 10 min at room temperature. Slides were prepared in quadruplicate from three patients per group. For each pair of slides, one was stained with a Diff-Quik kit, as the standard procedure, and the other one with 0.5% toluidine blue O solution (Fisher Scientific) for 5 min. Slides were analyzed on a BX-60 Olympus microscope equipped with an Olympus XC50 CCD camera with cellSens standard digital imaging software (Olympus Imaging Corp., Tokyo, Japan). A total of 423 cells were analyzed (n = 103 for control group; n = 150 for ZIKV; n = 170 for ZIKV/CZV) for qualitative and quantitative evaluation of morphological alterations. Keratinization was scored as initial too mild (cells showing initial signs of acidophilia at their surface or acidophilia detected in the peripheral cytoplasm) or moderate to severe (cells with a deep cytoplasm partially or fully acidophilic).

RESULTS

Clinical Features of the Patient Cohort

The study cohort was divided in three conditions: (1) Ctrl, infants with no infectious diseases nor neurological disorders without maternal ZIKV exposure; (2) Zikv, infants exposed to ZIKV with no microcephaly; (3) Zikv^{CZS}, infants exposed to ZIKV with microcephaly and clinical CZS symptoms. In both Zikv and Zikv^{CZS} conditions, the mothers were ZIKV positive during the first or second trimester of gestation and negative to other infectious agents (syphilis, toxoplasmosis, rubella, cytomegalovirus, and HIV). All groups were age and sex matched. Vision impairment consisting of macular atrophy, abnormal pigment deposition, optic disc excavation, and pallor were observed only for the three infants belonging to the Zikv^{CZS} condition at the time of sample collection. Two infants were affected bilaterally, and one was affected unilaterally (Table 1). Particularly, all infants included in this study are part of a multidisciplinary clinical follow up program currently in progress.[30] Clinical and demographic information is assembled in Tables 1 and 2.

Cellular Imprinting Proteomic Assay (CImPA) Development

To profile the ocular fingerprint in infants exposed to ZIKV, a cellular imprinting proteomics assay was developed, which combines the noninvasive impression cytology sample collection for enhanced cellular retrieval coupled with a streamlined optimized tryptic sample digestion to maximize protein/peptide recovery and label free quantitative bottom-up mass spectrometry (Figure 1). CImPA provided a broad proteome coverage, with a total of 2209 identified proteins (Figure S1A, Table S3) from which 865 were present in all samples (Figures S1B and S1C). The conjunctiva epithelial cell proteome showed a diverse distribution of biological processes and cellular compartments, being stimulus response and transport, membrane, and extracellular proteins among the most enriched ones (Figures S1D and S1E). Interestingly, six proteins make up 50% of the conjunctiva epithelium proteome content: lipocalin-1, lacritin, serum albumin, proline-rich protein 4, lysozyme, and mammaglobin-B (Figure 2A).

To assess the origin of the proteome retrieved by impression cytology, proteomes from different ocular fluids and tissues were compared.[36] The highest protein content overlap was observed with the RPE/choroid although vitreous humor, cornea, retina, and iris had around 70% of similar proteomes. Lens and aqueous humor proteomes had lowest overlap of only 28 and 18%, respectively (Figure 2B). A comparison of the conjunctiva epithelial proteome with the NEIBank for eye disease genes[37] revealed 66 genes associated with ocular diseases and 23 to other diseases (Figure 2C,D). Comparison between the CImPA proteome versus the brain-enriched and eye-extended proteome retrieved from the human protein atlas[38] revealed an overlap of 29 and 3 proteins, respectively (Figure 2E).

Although blood proteins were detected in conjunctival epithelial proteome, such as albumin, immunoglobulin, hemoglobin, apolipoprotein, serotransferrin, complement factors, and alpha-1-antitrypsin (Table S3), collectively, they make up less than 8% of the total protein content. There were 1579 common proteins to both conjunctiva surface and plasma (Human Plasma Peptide Atlas,[39] and 630 proteins unique to the ocular cells (Figure 2F). Certainly, the blood protein abundance did not hinder the identification of kinases, receptors, and transcription factors involved in several biological processes ranging from metabolism to intracellular signaling (Table S3).

CImPA Method Allows the Identification and Quantification of Ocular Surface Proteins in ZIKV-Infected Infants

Principal component analysis of all quantified ocular surface proteins obtained by CImPA showed discrete separation between the three conditions, infants with intrauterine Zika virus infection, with and without microcephaly at birth and controls (Figure S2A). Three comparisons were made to identify proteins differentially regulated between the Zikv^{CZS}, Zikv, and Ctrl conditions: (a) Zikv^{CZS} vs Ctrl, (b) Zikv vs Ctrl, and (c) Zikv^{CZS} vs Zikv (Figure 3A−C, Table 3, Tables S4−S6), which did not share the majority of regulated proteins (Figure 3D). Protein−protein interaction network analysis of the different comparisons revealed 70 and 14 reactome pathways enriched in the Zikv^{CZS} vs Ctrl and Zikv vs Ctrl comparisons, respectively (Figure S2B). The most enriched processes were associated with (a) immune system, (b) ocular dysfunctions, (c) interferon signaling, (d) cell death, (e) viral infection, and (f) neurological disorders (Figure 4). The immune system, neutrophil degranulation, visual phototransduction, metabolism of retinoids, interferon signaling, viral infection processes were mostly enriched in the Zikv^{CZS} vs Ctrl and Zikv^{CZS} vs Zikv comparisons.

https://dx.doi.org/10.1021/acs.jproteome.0c00320
J. Proteome Res. 2020, 19, 4496−4515

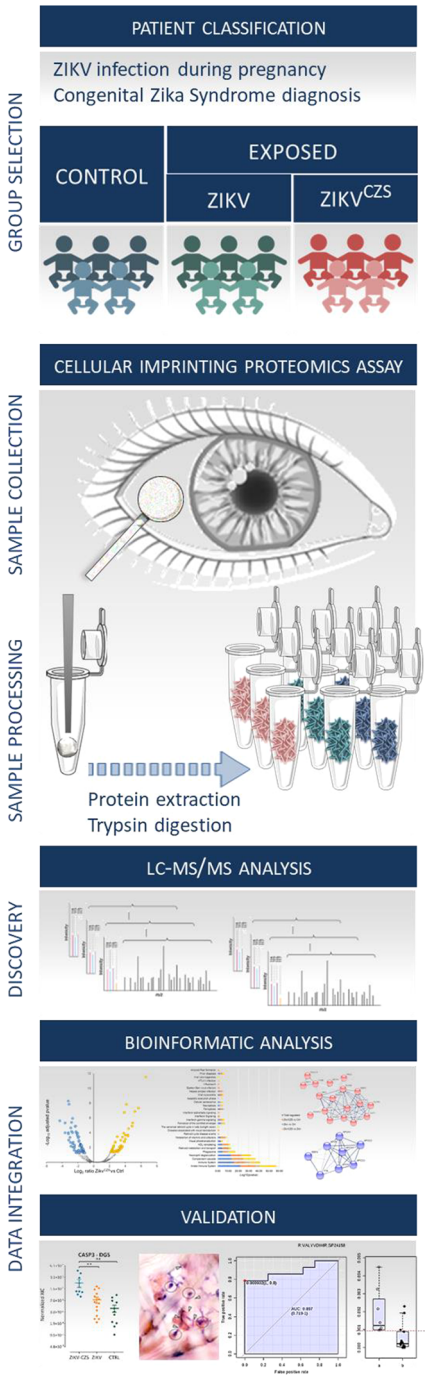

Figure 1. Cellular imprinting proteomics (CImPA) method applied to ocular surface alterations during congenital Zika syndrome. Experimental workflow of the CImPA method applied to a cohort of infants exposed to ZIKV during gestation with congenital Zika syndrome ($Zikv^{CZS}$ $n = 3$) and without congenital Zika syndrome (Zikv, $n = 5$) and age- and sex-matched controls (Ctrl, $n = 5$) (group selection). The sample collection was obtained using nitrocellulose filters used to capture the ocular surface epithelial cells and fluid (sample collection). Proteins were extracted from the membrane, digested, and analyzed by mass spectrometry (sample processing). Database search and statistical analysis were performed to identify differentially expressed proteins (discovery). Protein candidates were validated by parallel reaction monitoring, and microscopy analysis confirmed the presence of specific biological processes (data integration).

Neutrophil Degranulation Signature and Cell Death Activation in the Eye

Overall, the major changes in Zikv were activation of immune system (neutrophil degranulation), increased cell death primarily to proteins that are linked to neurological diseases. Across all the comparisons was the immune system response as the primary altered pathway (Figure 4) with 19 proteins increased in $Zikv^{CZS}$ compared to control specifically associated to neutrophil degranulation, suggestive of immune activation (Figure S2C). Indeed, a neutrophil protein signature based on neutrophil defensin 1 (DEFA1), neutrophil collagenase (MMP8), cytochrome *b*-245 heavy chain (CYBB), resistin (RETN), DnaJ homologue subfamily C member 5 (DNAJC5), olfactomedin-4 (OLFM4), eosinophil cationic protein (RNASE3), ADP-ribosyl cyclase/cyclic ADP-ribose hydrolase (BST1), protein S100-A12 (S100A12), neutrophil elastase (ELANE), azurocidin (AZU1), pentraxin-related protein (PTX3), chitotriosidase (CHIT1), bone marrow proteoglycan (PRG2), gamma-glutamyl hydrolase (GGH), chitinase-3-like protein 1 (CHI3L1), protein S100-A7 (S100A7), neutrophil cytosol factor 2 (NCF2), and myeloperoxidase (MPO) was found in $Zikv^{CZS}$ group (Figure 5). The upregulation of MPO, ELANE, ITGAM, RNASE3, AZU1, MMP8, PRTN3, DEFA1, and S100-A12 was validated by parallel reaction monitoring (Figure 5, Table S7). The interferon signaling pathways were enriched in the regulated proteins belonging to the $Zikv^{CZS}$ vs Ctrl comparison (Figure 4). IFIT3 protein was greatly increased, 38 times, in the $Zikv^{CZS}$ group compared to controls (Table S4).

Cell death pathways were enriched in the regulated proteins between the $Zikv^{CZS}$ and control and the Zikv and control conditions (Figure 4). Caspase-3 (CASP3) and BH3-interacting domain death agonist (BID) were differentially regulated in the $Zikv^{CZS}$ condition compared to controls being 3.5 and 4 times upregulated in the $Zikv^{CZS}$, respectively (Figure 6A,B). Moreover, gasdermin D was identified to be upregulated 6.5 times in the $Zikv^{CZS}$ condition at p-value < 0.01 and adjusted p-value < 0.07 during the discovery phase. Differential upregulation of gasdermin D in $Zikv^{CZS}$ compared to control was confirmed by parallel reaction monitoring of the ELCQLLLEGLEGVLR peptide, p-value = 0.04 (Figure 6C). Bright field microscopy of ocular epithelial cells isolated from ZIKV-infected children and control (Figure 6D) show clear morphological evidence of cell death such as pyknosis (Figure 6E), cytoplasmic vacuolization (Figure 6F), karyorrhesis (Figure 6G), karyolysis (Figure 6H), and disintegration of the nucleus (Figure 6I). A high percentage of cells with these morphologies were measured in Zikv and $Zikv^{CZS}$ conditions (Figure 6J).

Neurological diseases were among the statistically enriched processes found most enhanced in the $ZIKV^{CZS}$ compared to control (Figure 4). In our data set, proteins such as the afamin (AFM) and pigment epithelium-derived factor (PEDF or SERPINF1) were downregulated, while copine-1 and neuroblast differentiation-associated protein AHNAK were found upregulated in the $Zikv^{CZS}$ vs Ctrl (Table S6). PRM analysis confirmed CPNE1, AHNAK, and DAG1 were significantly upregulated (Figure 7A–C), while CLEC3B were significantly downregulated (Figure 7D) in both the $Zikv^{CZS}$ vs Ctrl and $Zikv^{CZS}$ vs Zikv comparisons. Only AHNAK (Figure 7C) and BASP1 (Figure 7E) were regulated in Zikv vs Ctrl comparison (Table S5).

https://dx.doi.org/10.1021/acs.jproteome.0c00320
J. Proteome Res. 2020, 19, 4496–4515

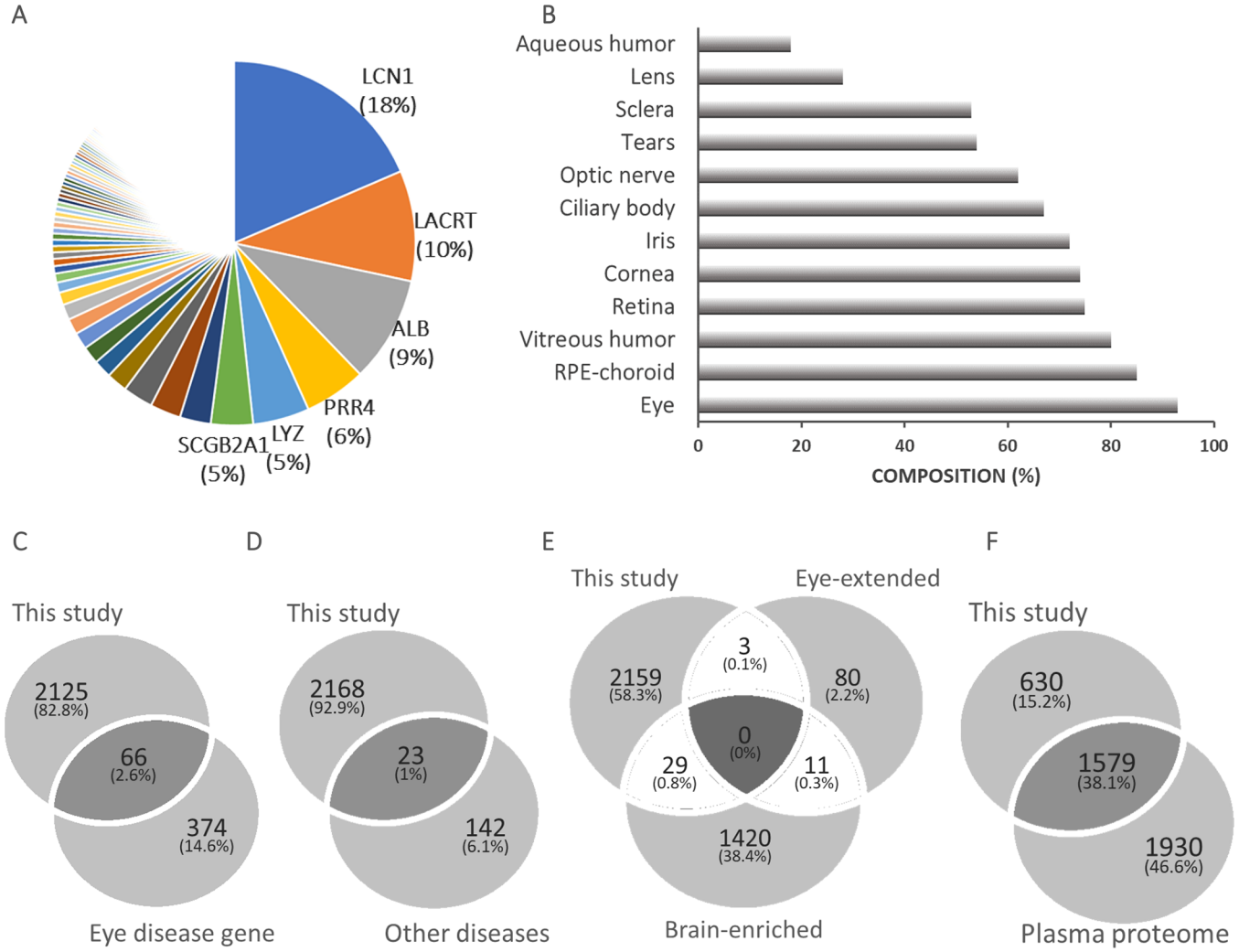

Figure 2. CImPA enables the proteome assessment of different ocular compartments and fluids. Abundance of proteins identified in the epithelial cells and fluid extracted using the impression cytology technique. Intensity-based absolute quantification (iBAQ)[113] was used to calculate the intrasample protein abundance, and the proteins were ranked based on their abundance (A). Distribution of proteins identified using the impression cytology method in this study according to the proteome of different ocular tissues and fluids (tears, aqueous humor, lens, vitreous humor, retina, and retinal pigment epithelium (RPE)/choroid as described by Ahmad et al.[36] (B). Comparison of proteins identified using the impression cytology method in this study and genes involved in eye diseases reported in the NEIBank database (C). Comparison of proteins identified using the impression cytology method in this study and genes identified in the eye compartments involved in other diseases as reported in the NEIBank database (D). Comparison of proteins identified using the impression cytology method in this study and brain and eye-enriched proteins reported in the Human Protein Atlas database (E). Comparison of proteins identified using the impression cytology method in this study and the human plasma proteome, according to Schwenk et al.[39] (F).

Differential Regulation of Proteins Associated to Ocular Diseases

Decreased protein expression assessed by CImPA belonged to key cellular pathways with retinoid metabolism dominating in Zikv^{CZS} compared to controls (Figure 4). Several proteins belonging to this pathway were validated by PRM (Figure 8A–D and Table S7). For example, retinol-binding protein 4 (RBP4) was decreased by more than 50 times in Zikv^{CZS} compared to control (see representative RBP4 peptide (YWGVASFLQK) in Figure 8B) Furthermore, six apolipoproteins (APOA1, APOA2, APOA4, APOB, APOC2, and APOC3) were decreased in Zikv^{CZS} compared to controls (Figure S2D). APOB was downregulated three times in the Zikv^{CZS} condition (Table S4). The upregulation of aldehyde dehydrogenase dimeric NADP-preferring (ALDH3A1) in the Zikv^{CZS} and Zikv conditions compared to controls could be related to the eye protection against oxidative damage. Alcohol dehydrogenase 1B (ADH1B) was identified downregulated in the Zikv^{CZS} compared to control condition (Figure 8C). Proteins associated to the cornified envelope were regulated in the three comparisons. The CImPA method allowed the quantification of 30 mammalian cellular keratin proteins (see Table S3 for full list). But interestingly, a different regulation pattern of intermediate filament proteins, the keratins, was identified in the Zikv^{CZS} vs Ctrl (KRT15 and 23), Zikv vs Ctrl (KRT3, 6B, 16, 23, 31 and 76), and Zikv^{CZS} vs Zikv (3, 6B, 16, 23, 31, 76 and 85) (Tables S4–S6). Reflecting the proteomics findings, quantitative analysis by bright field microscopy of conjunctival epithelial cells obtained by impression cytology from children with CZS show a higher degree of moderate to severe keratinization, while initial to moderate keratinization can be observed in the Zikv group, and the control group presented fewer cells displaying any level of this process (Figure 8E).

https://dx.doi.org/10.1021/acs.jproteome.0c00320
J. Proteome Res. 2020, 19, 4496–4515

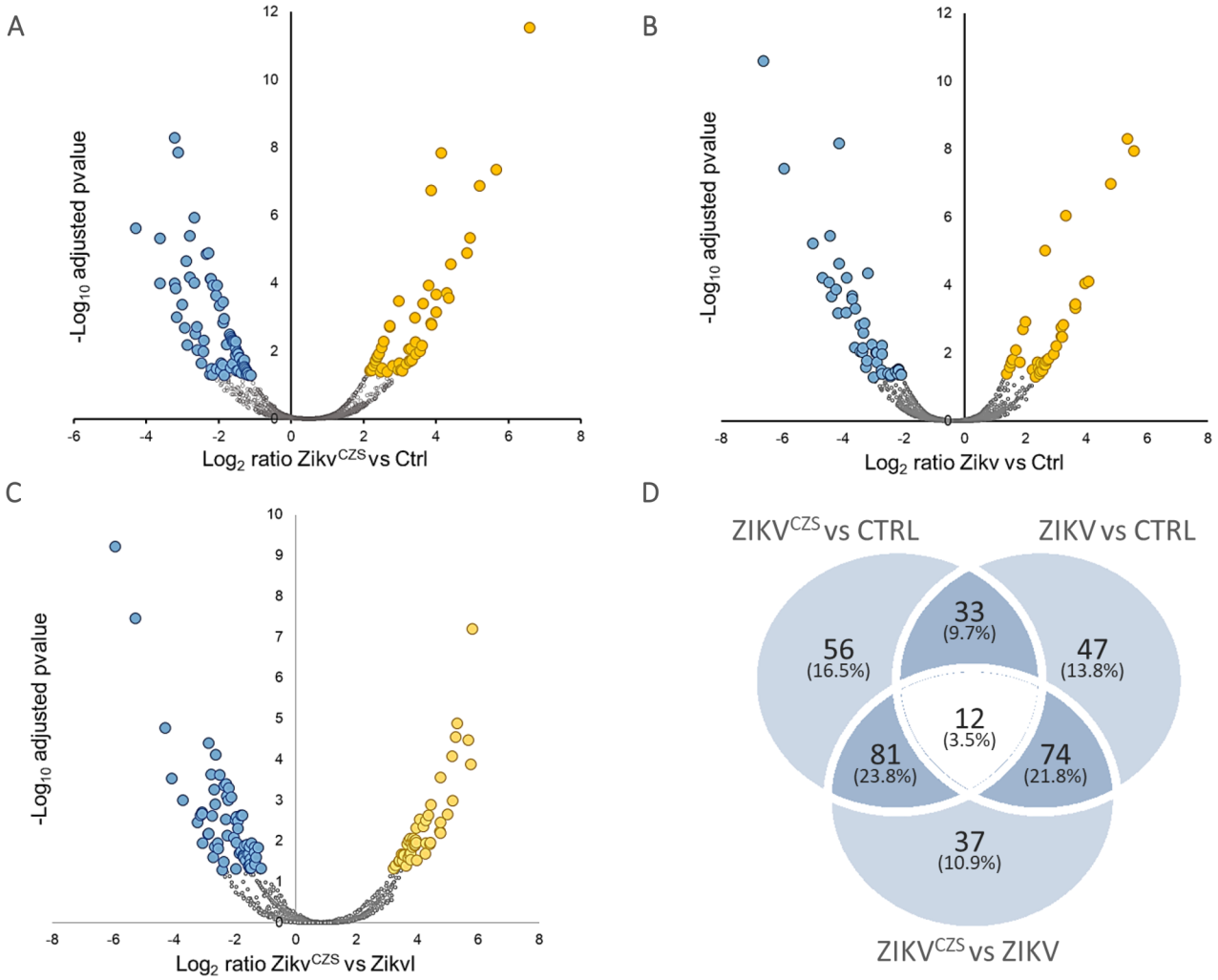

Figure 3. Differentially regulated proteins and pathways modulated in Zikv^{CZS}, Zikv, and Ctrl conditions. Zikv^{CZS} vs Ctrl (A), Zikv vs Ctrl (B), and ZikvCZS vs Zikv (C). Proteins with adjusted p-value < 0.05 were considered statistically significant. Overlap between the differentially regulated proteins in the three comparisons (D).

Table 3. Three Comparisons Were Made To Identify Proteins Differentially Regulated between the Zikv^{CZS}, Zikv, and Ctrl Conditions: (a) Zikv^{CZS} vs Ctrl, (b) Zikv vs Ctrl, and (c) Zikv^{CZS} vs Zikv[a]

differentially regulated (adjusted p-value ≤ 0.05)	protein no.		
	total	upregulated	downregulated
Zikv^{CZS} vs Ctrl Figure 2A, Table S3	182	82	100
Zikv vs Ctrl Figure 2B, Table S4	166	70	96
Zikv^{CZS} vs Zikv Figure 2C, Table S5	204	110	94

[a]The analysis revealed proteins differentially regulated with adjusted p-value ≤0.05 (Figure 3A−C, Tables S2−S4).

Infants Exposed to ZIKV Infection during Gestation and without CZS Harbor Differential Ocular Surface Proteome

The ocular surface proteome of the Zikv group compared to controls showed the regulation of 166 proteins (Figure 3B and Table S5). The number of enriched Reactome pathways and their significance had lower p-values compared to the Zikv^{CZS} vs control comparison (Figure S2B). Immune system response, cell death and cornified envelope proteins were enriched. For the immune response pathway, the IFIT3 protein was upregulated 17 times in the Zikv compared to Ctrl (Table S5). The upregulation of IFIT3 was confirmed by PRM using the ATMYNLLAYIK peptide in the Zikv group (p-value = 0.03), (Table S2). Moreover, interferon-induced helicase C domain-containing protein 1 (IFIH1) was upregulated 27 times in the Zikv group compared to Ctrl (Table S5). Quantitative validation using PRM analysis of selected protein candidates identified HIST1H1D and BASP1 as discriminating proteins for the Zikv vs Ctrl conditions with AUC > 0.8 (Table 5). These proteins were decreased in the Zikv condition compared to control (Table S7). None of the children exposed to ZIKV without CZS had visual impairment at the time of collection. However, significant molecular alterations were detected in the eyes of infants exposed to ZIKV.

Validation of Differentially Regulated Proteins Involved in Immune Response, Ocular Disorders, Cell Death, and Neurological Diseases

To validate the quantification of identified by CImPA, we chose 26 proteins to develop a targeted PRM assay (Table S2 and S7) including ALDH3A1, AZU1, BID, CASP3, CLEC3B, CPNE1, DMBT1, EPS8L2, ITGAM, KRT13, MMP8, MPO, RBP4, and

https://dx.doi.org/10.1021/acs.jproteome.0c00320
J. Proteome Res. 2020, 19, 4496−4515

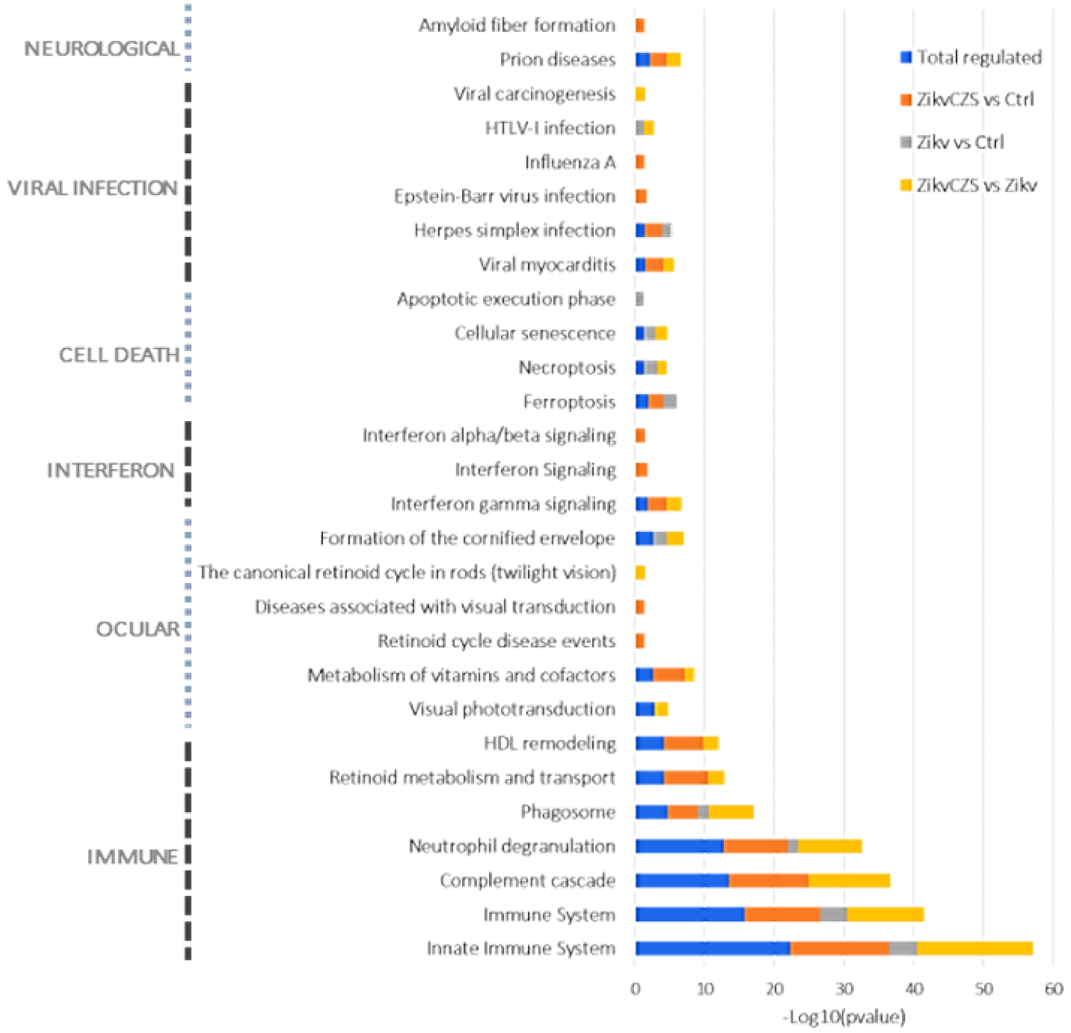

Figure 4. Pathways enriched in the different data sets (total regulated, Zikv^{CZS} vs Ctrl, Zikv vs Ctrl, and Zikv^{CZS} vs Zikv) and grouped into immune system, ocular disorders, interferon signaling, cell death, viral infection, and neurological diseases. The −Log10 of the adjusted *p*-value for each comparison is defined by the length of the corresponding bar.

RNASE3, HIST1D, BASP1, and PRTN as potential discriminative features that distinguish Zikv compared to control (Tables 4 and 5). As well, we included proteins that differentiated between the Zikv^{CZS} vs Zikv such as AHNAK, AZU1, CASP3, DEFA1, DMBT1, ELANE, ITGAM, MPO, PRTN3, RETN, RNASE3, and S100A12, as potential discriminative markers (Table 6). The above-mentioned discriminative peptides showed AUC greater than 0.8, obtained by univariate ROC curve analysis.

DISCUSSION

Here, we present a new proteomic workflow, CImPA, which is based on the optimized impression cytology procedure[31] and coupled to integrated MS-based quantitative proteomics. Using CImPA, we were able to define the proteome composition of the ocular epithelial surface proteome and its modulation in pathophysiological conditions. A key aspect of the workflow is impression cytology, which is a non- or minimally invasive technique to diagnose and understand molecular alterations in ocular diseases and allows the collection of live cells,[31] being used to evaluate ocular surface abnormalities in systemic diseases such as diabetes, cystic fibrosis and celiac disease.[40−42] One seminal work on impression cytology and proteomics used 2D-DIGE approach to investigate the ocular dysfunctions in patients with meibomian gland dysfunction and dry eye disease was published.[43] In our method, protein extraction is based on SDC, a trypsin and MS-compatible detergent, which allowed a streamlined approach using a single step, which should reduce protein loss but allows direct intersection with LC/MS. Large-scale quantitative proteomics using nLC-MS/MS allowed us to identify 2062 proteins with high confidence (compared to 348 by 2D-DIGE). Intrasample quantitative analysis of the ocular proteome revealed that six proteins (lipocalin-1, lacritin, serum albumin, proline-rich protein 4, lysozyme, and mammaglobin-B) constituted 50% of the total amount of the ocular epithelial proteome. Lipocalin, lacritin, and lysozyme are also involved in host response to infections. Lipocalin-1 (LCN1, human tears lipocalin) and neutrophil gelatinase-associated lipocalin (LCN2) were among the top 100 most abundant proteins in the ocular surface proteome (Figure 2A). Lipocalins are extracellular proteins and belong to the lipocalin superfamily that bind and transport hydrophobic compounds such as lipids, hormones and vitamins. LCN1 binds phospholipids and retinol[44] and is expressed mainly in the lachrymal and salivary glands. LCN2 binds preferentially iron and is expressed mainly in the bone marrow.[45] Moreover, LCN1 and LCN2 mediate

https://dx.doi.org/10.1021/acs.jproteome.0c00320
J. Proteome Res. 2020, 19, 4496−4515

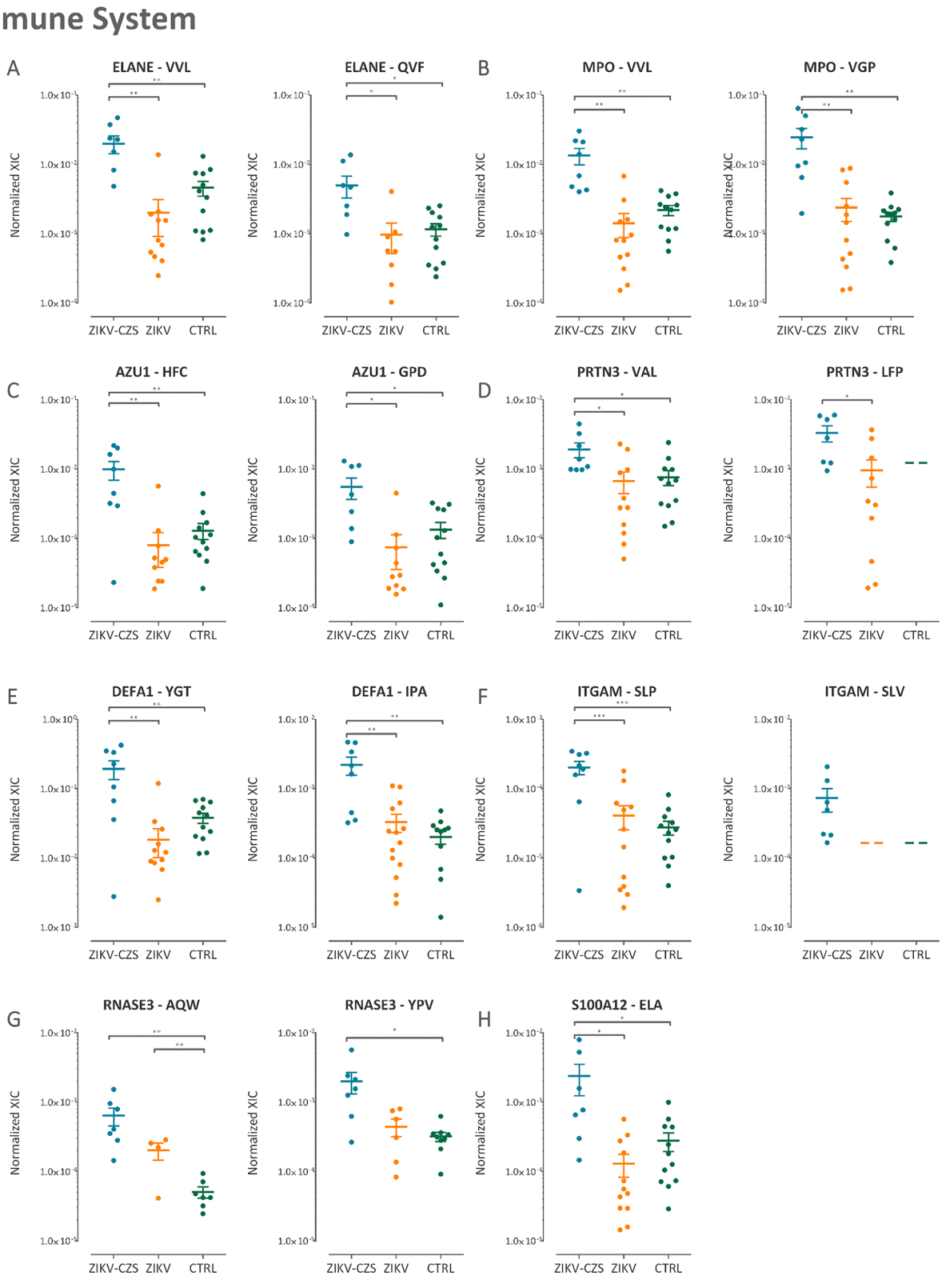

Figure 5. ZIKV modulates immune system pathway in the ocular surface proteome. Differentially regulated proteins belonging to the immune system pathway identified during the discovery phase and validated by PRM. The monitored peptide abundance is reported for the Zikv^{CZS}, Zikv, and Ctrl groups for the proteins Neutrophil elastase, ELANE (A), myeloperoxidase, MPO (B), azurocidin, AZU1 (C), myeloblastin, PRTN3 (D), neutrophil defensin, DEFA1 (E), integrin alpha-M, ITGAM (F), eosinophil cationic protein, RNASE3 (G) and S100A12 (H) (* < 0.05, ** < 0.01, and *** < 0.001).

immune and inflammatory response against microbial and fungal infections.[46−48] Interestingly, LCN1 was the most abundant protein within the total proteins identified, contributing to 18% of the total protein abundance. Dota A. et al. showed

https://dx.doi.org/10.1021/acs.jproteome.0c00320
J. Proteome Res. 2020, 19, 4496−4515

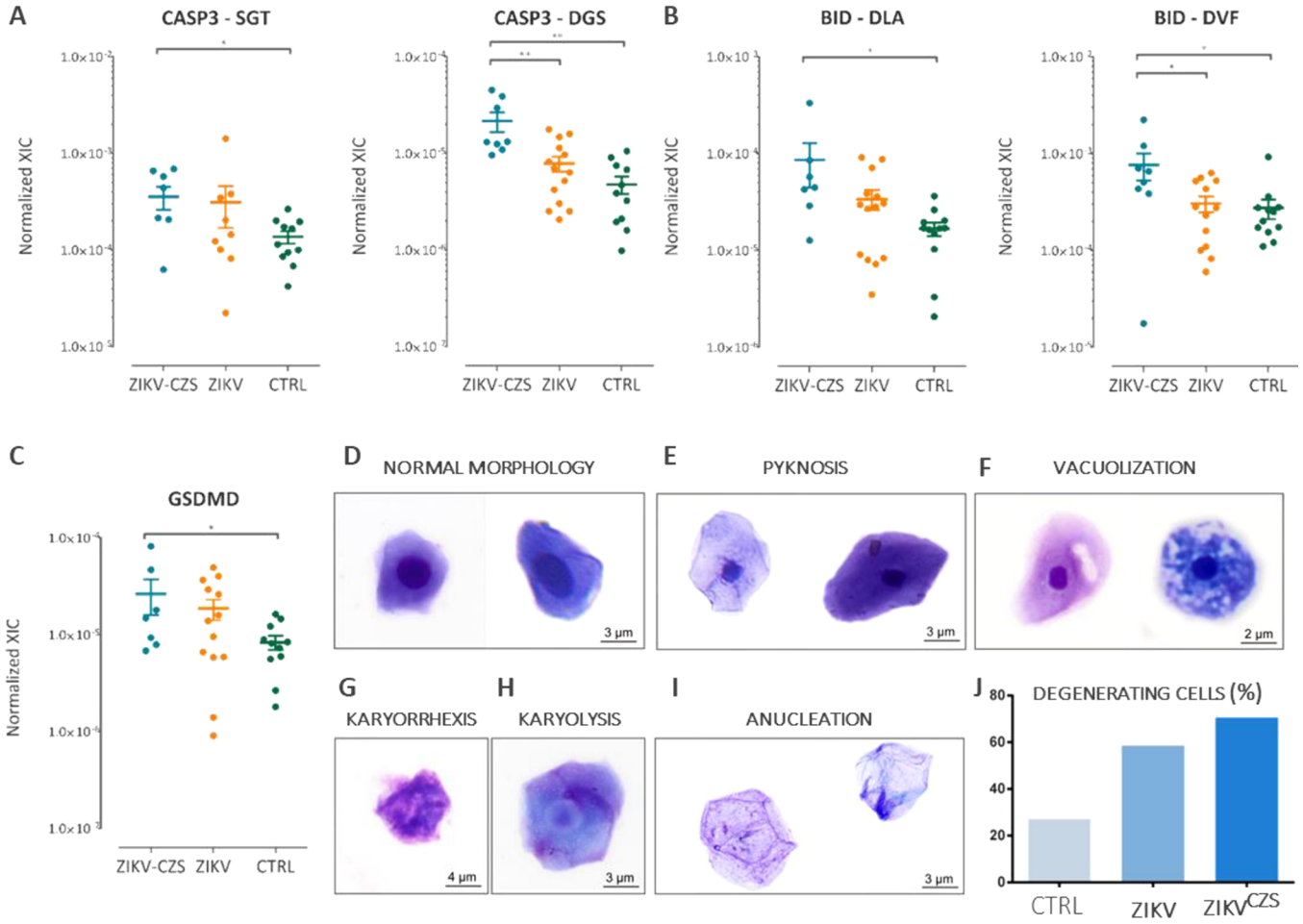

Figure 6. ZIKV promotes cellular degeneration/cell death. Differentially regulated proteins belonging to the cell death pathway identified during the discovery phase and validated by PRM. The monitored peptide abundance is reported for the Zikv^{CZS}, Zikv, and Ctrl groups for the proteins: Caspase-3 (A), BH3-interacting domain death agonist (B), and gasdermin (C). * < 0.05, ** < 0.01, and *** < 0.001. Representative cells from uninfected group show normal morphology (D). Nuclear and cytoplasmic alterations observed in cells collected from ZIKV (infected with no clinical signs) (D, left panel; F, G, and H, left panel) or ZIKV^{CZS} (diagnosed congenital Zika syndrome (E, right panel; F, G, H, and I, right panel) children. Quantitative analyses show increased number of conjunctival cells with morphological signs of degeneration/cell death. Cells were collected by impression cytology, centrifuged, and stained with Diff-Quik or toluidine blue (J). A total of 423 cells were counted and scored for morphological changes.

that LCN2 was a conjunctiva epithelium-specific gene.[49] The difference could be due to the collection method. Indeed, compared to our improved impression cytology approach, brush cytology was used to obtain conjunctival epithelium, a method that collects all epithelial cell layers of the conjunctival epithelium.[49] Comparison with the proteome of other ocular tissues and fluids revealed high similarity with the RPE/choroid and less similarity with lens and aqueous humor.

The CImPA method proved data to map the ocular surface proteome of infants exposed to ZIKV infection with and without CZS compared controls, although impression cytology has been used to detect superficial viral infections such herpes simplex virus, varicella zoster virus, and adenovirus.[50] We searched for Zika virus proteins in the ocular surface proteome, and no viral proteins were detected in these samples (data not shown). However, the presence of ZIKV antigens was detected in the ocular tissue samples from four deceased fetuses with a diagnosis of CZS using a ZIKV NS2B protein antibody.[24] The antigen was detected in the iris, neural retina, and the optic nerve. Moreover, RT-PCR analysis of the aqueous sample from a Brazilian man with ZIKV infection was positive, and ZIKV was identified in conjunctival swabs obtained from six patients with ZIKV infection.[51] In our data, ZIKV proteins were not detected using the CImPA method. This could be due to the eye region sampled and the low abundance of viral proteins compared to host proteins. Moreover, the infants were infected in the first trimester of gestation and at the time of sample collection the viremia could have been drastically decreased. Nonetheless, proteins differentially regulated between the different comparisons revealed the modulation of pathways involved in immune system response, cell death, and ocular and neurological dysfunctions. Proteins associated with immune system response and neutrophil degranulation were upregulated in the Zikv^{CZS} and Zikv compared to the Ctrl condition. The upregulation of neutrophil-associated proteins during flavivirus infection has been shown.[52,53] Neutrophil defensin-1 belongs to the defensins family present in the neutrophil granules with activity against bacteria, fungi, parasites, and viruses.[54,55] DEFA1 was found

https://dx.doi.org/10.1021/acs.jproteome.0c00320
J. Proteome Res. 2020, 19, 4496−4515

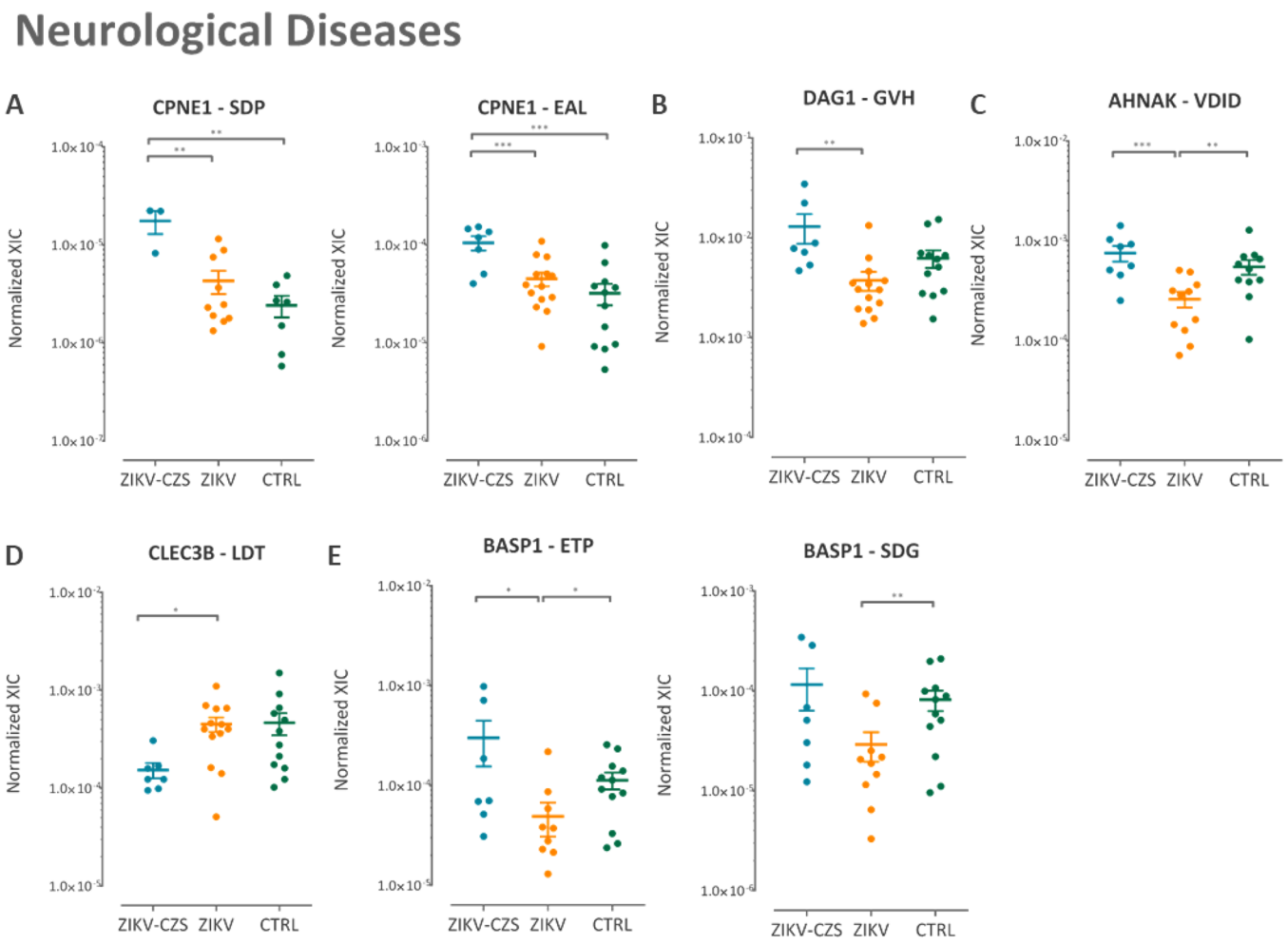

Figure 7. ZIKV exposure modulates proteins associated to neuronal disorders. Differentially regulated proteins belonging to the neurological disease pathway identified during the discovery phase and validated by PRM. The monitored peptide abundance is reported for the Zikv^{CZS}, Zikv, and Ctrl groups for the proteins: copine-1 (A), dystroglycan (B), neuroblast differentiation-associated protein AHNAK (C), tetranectin (D), and brain acid soluble protein 1 (E), * < 0.05, ** < 0.01, and *** < 0.001.

upregulated in the cerebrospinal fluid of patients infected with West Nile virus with neuroinvasive complications[56] and also in the blood of Dengue-infected children with hemorrhagic fever.[57] Myeloperoxidase activity and expression was elevated in mice infected by the intracranial route by DENV-3 confirming the neutrophil infiltration.[58] Moreover, MPO was released by neutrophils collected from mice infected with Japanese encephalitis virus.[53] A transcriptomic analysis of peripheral blood mononuclear cells isolated from children with acute-phase Dengue hemorrhagic fever revealed an activation of the S100A12 protein.[59]

As observed for West Nile virus, herpes simplex virus-1, and ebola virus, Zika virus has tropism for immunoprivileged organs like the brain and the eye.[60,61] The infection and persistence in these organs pose new challenges in understanding the dynamics of viral spreading, life cycle and clearance. Neutrophils are essential effectors of the innate immune response. Their recruitment in an infected tissue is a host-defense mechanism that can induce tissue damage if not finely regulated. Infection of neonatal C57BL/6 wild-type mice at 1 day post birth with ZIKV showed that the virus infects the cornea and retina resulting in chorioretinal lesions.[62] The infection is followed by inflammatory cells infiltration and increased local expression of chemokines. In ZIKV-infected patients, there is an increased cellular infiltration and inflammation.[24,63] Inflammation in the eye was found in other arbovirus infections, and disease management was achieved through topical and systemic corticosteroid treatment.[64−66] Neutrophil degranulation pathway was found to be activated in the conjunctival epithelial cells retrieved from ZIKV-infected children with CZS. This pathway is associated with neutrophils migration toward the inflammatory site mobilizing granules with antimicrobial properties. Moreover, neutrophils secrete inflammatory cytokines and mediators stimulating T-cells. Immune activation has been associated with inflammatory and degenerative eye diseases such as adult macular degeneration and uveitis.[67] In the brain of infected mice, neutrophils and mononuclear cells were infiltrated, and polymorphonuclear cells (PMNs) were detected near blood vessel.[68] Neutrophil and eosinophil infiltration has been described in several ocular pathologies such as ocular Stevens-Johnson syndrome, mucous membrane pemphigoid, Wegener's granulomatosis, and cicatricial pemphigoid.[69−72] Microscopy analysis of the cells content of membranes retrieved from the Zikv and Zikv^{CZS} conditions revealed an increase in immune cells infiltrates associated with an activated ocular surface inflammatory response to ZIKV infection. In particular, we show the overexpression of neutrophils and eosinophil granule constituents correlated to the activation of neutrophil

https://dx.doi.org/10.1021/acs.jproteome.0c00320
J. Proteome Res. 2020, 19, 4496−4515

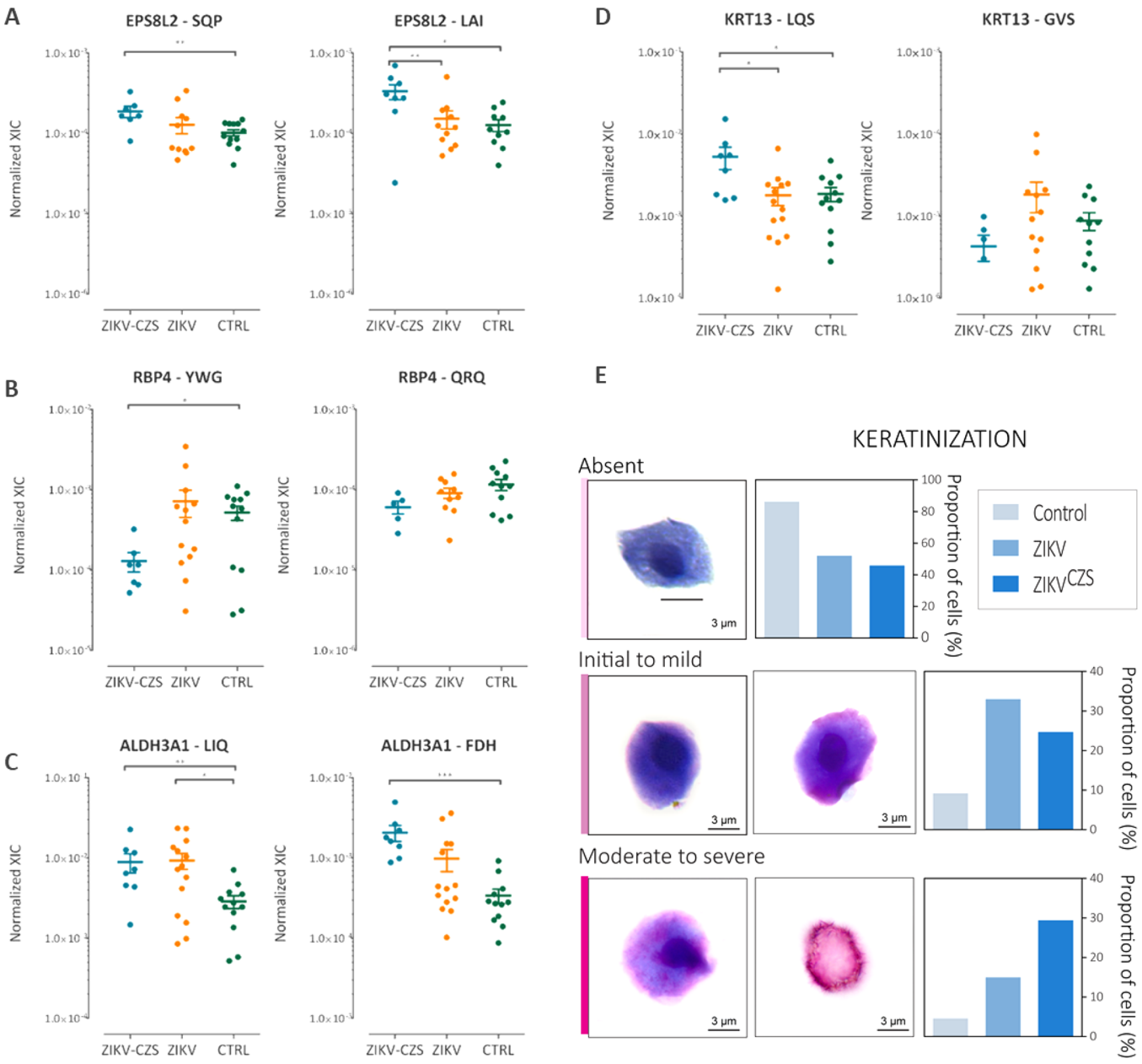

Figure 8. ZIKV impacts the expression of proteins involved in ocular disorders in infants with and without CZS. Differentially regulated proteins belonging to the ocular disorder pathway identified during the discovery phase and validated by PRM. The peptide abundance is reported for the Zikv^{CZS}, Zikv and Ctrl groups for proteins: Epidermal growth factor receptor kinase substrate 8-like protein 2 (A), retinol-binding protein 4 (B), aldehyde dehydrogenase (C) and keratin, type I cytoskeletal 1 (D). Representative images and quantitative morphological analyses of cells collected from children with ZIKV (infected with no clinical signs), ZIKV/CZV (diagnosed congenital Zika syndrome) or uninfected controls using impression cytology. Cytocentrifuged preparations were stained with Diff-Quik (E). A total of 423 cells were counted and scored for morphological signs of keratinization.

degranulation process in Zikv and Zikv^{CZS} children compared to controls. It is unclear if the immune cells infiltration would be the indirect cause of chorioretinal lesions or if the ZIKV itself elicits these eye abnormalities or a combination of the two phenomena.

Cell death is another critical process in the pathophysiology of eye diseases found activated in infants exposed to ZIKV infection. Likewise, age-related macular degeneration is also linked to cell death, both apoptosis and pyroptosis. In this disease, there are elevated tissue quantities of cleaved caspase-3 and gasdermin D in RPE-choroid tissues.[73] Pterygium, a common ocular disease characterized by proliferating fibrovascular tissue, also displays pyroptosis in the pathological process of formation and progression.[74] The upregulation of gasdermin-D, caspase-3, and BID in the eyes of infants exposed to Zikv during gestation indicates an increase in ocular cell death, which stresses the need for regular ophthalmological follow-up of exposed children, even without any initial sign of CZS.

Our study showed the dysregulation of proteins involved in ocular processes, including the metabolism of retinoids, which is

https://dx.doi.org/10.1021/acs.jproteome.0c00320
J. Proteome Res. 2020, 19, 4496−4515

Table 4. Selective Peptides Monitored by PRM for Zikv^{CZS} and Control Comparison (AUC Greater than 0.8)[a]

Zikv^{CZS} vs Ctrl	AUC	description
AHNAK - AVE	0.812	Neuroblast differentiation-associated protein AHNAK. May be required for neuronal cell differentiation
AHNAK - VDIS	0.812	
ALDH3A1 - FDH	0.989	Aldehyde dehydrogenase. Involved in the metabolism of corticosteroids, biogenic amines, neurotransmitters, and lipid peroxidation. May play a role in preventing corneal damage caused by ultraviolet light.
ALDH3A1 - LIQ	0.854	
AZU1 - HFC	0.864	Azurocidin. This is a neutrophil granule-derived antibacterial and monocyte- and fibroblast-specific chemotactic glycoprotein.
BID - DVF	0.823	BH3-interacting domain death agonist. Counters the protective effect of Bcl-2.
CASP3 - DGS	0.989	Caspase-3. Involved in the activation cascade of caspases responsible for apoptosis execution. Triggers cell adhesion in sympathetic neurons through RET cleavage.
CLEC3B - LDT	0.854	Tetranectin binds to plasminogen and to isolated kringle 4. May be involved in the packaging of molecules destined for exocytosis.
CPNE1 - EAL	0.812	Copine-1. Calcium-dependent phospholipid-binding protein that plays a role in calcium-mediated intracellular processes. Plays a role in neuronal progenitor cell differentiation; induces neurite outgrowth via an AKT-dependent signaling cascade.
DEFA1 - IPA	0.958	Neutrophil defensin 1. Defensins are thought to kill microbes by permeabilizing their plasma membrane
DMBT1 - FGQ	0.812	Deleted in malignant brain tumors 1 protein. Required for terminal differentiation of columnar epithelial cells during early embryogenesis. Binds to HIV-1 envelope protein and has been shown to both inhibit and facilitate viral transmission.
DMBT1 - FIS	0.833	
ELANE - VVL	0.802	Neutrophil elastase. Modifies the functions of natural killer cells, monocytes, and granulocytes. Inhibits C5a-dependent neutrophil enzyme release and chemotaxis
EPS8L2 - LAI	0.875	Epidermal growth factor receptor kinase substrate 8-like protein 2.
ITGAM - SLP	0.864	Integrin alpha-M. Integrin ITGAM/ITGB2 is implicated in various adhesive interactions of monocytes, macrophages, and granulocytes as well as in mediating the uptake of complement-coated particles and pathogens.
ITGAM - SLV	0.937	
KRT13 - LQS	0.823	Keratin, type I cytoskeletal 1.
MMP8 - DAF	0.859	Neutrophil collagenase. Can degrade fibrillar type I, II, and III collagens.
MPO - VGP	0.942	Myeloperoxidase. Part of the host defense system of polymorphonuclear leukocytes.
MPO - VVL	0.989	
PRTN3 - LPF	0.937	Myeloblastin. Serine protease that degrades elastin, fibronectin, laminin, vitronectin, and collagen. By cleaving and activating receptor F2RL1/PAR-2, enhances endothelial cell barrier function and thus vascular integrity during neutrophil transendothelial migration.
PRTN3 - VAL	0.833	
RBP4 - QRQ	0.817	Retinol-binding protein 4. Retinol-binding protein that mediates retinol transport in blood plasma. Delivers retinol from the liver stores to the peripheral tissues. Transfers the bound all-trans retinol to STRA6, which then facilitates retinol transport across the cell membrane
RETN - AIS	0.812	Resistin. Promotes chemotaxis in myeloid cells.
RETN - IQE	0.843	
RNASE3 - AQW	0.901	Eosinophil cationic protein. Cytotoxin and helminthotoxin with low-efficiency ribonuclease activity.
RNASE3 - YPV	0.812	

[a]AUC obtained by univariate ROC curve analysis (Metaboanalyst v4.0). Description based on UniProt protein function description (https://www.uniprot.org/).

essential for vision[75] and was downregulated in Zikv^{CZS} compared to controls. Such dysregulation has been associated with several ocular diseases such as Stargardt disease, autosomal recessive cone-rod dystrophy, autosomal recessive childhood-onset severe retinal dystrophy, Leber congenital amaurosis, and autosomal recessive retinitis punctata albescens.[76−79] Zikv^{CZS} infants showed downregulation of RBP4, a 21 kDa protein synthesized primarily in the liver and other tissues such as retinal pigment epithelium and choroidal plexus brain.[80,81] It belongs to the lipocalin superfamily, and the main function is to bind retinol (vitamin A_1) in hepatocytes and deliver it to peripheral tissues.[82] Retinol, in the form of retinal, is essential for the visual cycle and defects in RBP4 expression have been associated with ocular diseases. In human patients, iris coloboma, atrophy, or focal loss of the retinal pigment epithelium (RPE) and the choroid has been associated with a homozygous splice site variant (c.111 + 1G > A) and heterozygous missense mutations (Ile41Asn and Gly75Asp) in the gene encoding RBP4 and its consequent serum level reduction.[83,84] Mice lacking RBP4 had impaired visual function and transgenic expression of human RBP4 induced normal electro-retinogram and retinol metabolism.[85−87] Also linked to the retinol metabolism, six apolipoproteins were downregulated in the Zikv^{CZS} condition compared to control. Recently, ApoA-I has been identified as an all-*trans*-retinoic acid-binding protein secreted by the choroid and sclera tissues.[88] Several proteins involved in the cornified epithelium envelope were identified to be altered between exposed infants versus control, suggesting the break of the cornified cell envelope that constitutes a protective barrier of squamous epithelial cells.[89] In skin keratinocytes, cornified cell

https://dx.doi.org/10.1021/acs.jproteome.0c00320
J. Proteome Res. 2020, 19, 4496−4515

Table 5. Selective Peptides Monitored by PRM for Zikv and Control Comparison (AUC Greater than 0.8)[a]

Zikv vs Ctrl	AUC	description
HIST1H1D - ALA	0.934	Histone H1 protein binds to linker DNA between nucleosomes forming the macromolecular structure known as the chromatin fiber.
HIST1H1D - ASG	0.880	
AHNAK - VDIS	0.875	Neuroblast differentiation-associated protein AHNAK. May be required for neuronal cell differentiation.
PRTN3 - LPF	0.857	Myeloblastin. Serine protease that degrades elastin, fibronectin, laminin, vitronectin, and collagen. By cleaving and activating receptor F2RL1/PAR-2, enhances endothelial cell barrier function and thus vascular integrity during neutrophil transendothelial migration.
BASP1 - ETP	0.845	Brain acid soluble protein 1. Neuronal axonal membrane protein NAP-22
BASP1 - SDG	0.839	
ELANE - VVL	0.833	Neutrophil elastase. Modifies the functions of natural killer cells, monocytes and granulocytes. Inhibits C5a-dependent neutrophil enzyme release and chemotaxis.
DEFA1 - YGT	0.827	Neutrophil defensin 1. Defensins are thought to kill microbes by permeabilizing their plasma membrane
RETN - AIS	0.827	Resistin. Promotes chemotaxis in myeloid cells.

[a]AUC obtained by univariate ROC curve analysis (Metaboanalyst v4.0). Description based on UniProt protein function description (https://www.uniprot.org/).

Table 6. Selective Peptides Monitored by PRM for $Zikv^{CZS}$ and Zikv Comparison (AUC Greater than 0.8)[a]

$Zikv^{CZS}$ vs Zikv	AUC	description
AHNAK - VDID	0.928	Neuroblast differentiation-associated protein AHNAK. May be required for neuronal cell differentiation
AHNAK - VDT	0.861	
ALDH3A1 - FDH	0.803	Aldehyde dehydrogenase. Involved in the metabolism of corticosteroids, biogenic amines, neurotransmitters, and lipid peroxidation. May play a role in preventing corneal damage caused by ultraviolet light.
AZU1 - GPD	0.857	Azurocidin. This is a neutrophil granule-derived antibacterial and monocyte- and fibroblast-specific chemotactic glycoprotein.
AZU1 - HFC	0.892	
CASP3 - DGS	0.839	Caspase-3. Involved in the activation cascade of caspases responsible for apoptosis execution. Triggers cell adhesion in sympathetic neurons through RET cleavage.
CLEC3B - LDT	0.825	Tetranectin binds to plasminogen and to isolated kringle 4. May be involved in the packaging of molecules destined for exocytosis.
DAG1 - GVH	0.812	Dystroglycan. The dystroglycan complex is involved in a number of processes including laminin and basement membrane assembly, sarcolemmal stability, cell survival, peripheral nerve myelination, nodal structure, cell migration, and epithelial polarization.
DEFA1 - IPA	0.892	Neutrophil defensin 1. Defensins are thought to kill microbes by permeabilizing their plasma membrane
DEFA1 - YGT	0.883	
DMBT1 - FGQ	0.875	Deleted in malignant brain tumors 1 protein. Required for terminal differentiation of columnar epithelial cells during early embryogenesis. Binds to HIV-1 envelope protein and has been shown to both inhibit and facilitate viral transmission.
DMBT1 - FIS	0.875	
ELANE - QVF	0.892	Neutrophil elastase. Modifies the functions of natural killer cells, monocytes and granulocytes. Inhibits C5a-dependent neutrophil enzyme release and chemotaxis.
ELANE - VVL	0.883	
EPS8L2 - LAI	0.830	Epidermal growth factor receptor kinase substrate 8-like protein 2.
HIST1H1D - ALA	0.901	Histone H1 protein binds to linker DNA between nucleosomes forming the macromolecular structure known as the chromatin fiber.
ITGAM - SLP	0.883	Integrin alpha-M. Integrin ITGAM/ITGB2 is implicated in various adhesive interactions of monocytes, macrophages and granulocytes as well as in mediating the uptake of complement-coated particles and pathogens.
ITGAM - SLV	0.937	
KRT13 - LQS	0.812	Keratin, type I cytoskeletal 1.
MPO - VGP	0.946	Myeloperoxidase. Part of the host defense system of polymorphonuclear leukocytes.
MPO - VVL	0.973	
PRTN3 - LPF	0.803	Myeloblastin. Serine protease that degrades elastin, fibronectin, laminin, vitronectin, and collagen. By cleaving and activating receptor F2RL1/PAR-2, enhances endothelial cell barrier function and thus vascular integrity during neutrophil transendothelial migration.
PRTN3 - VAL	0.883	
RETN - AIS	0.946	Resistin. Promotes chemotaxis in myeloid cells
RETN - IQE	0.919	
RNASE3 - AQW	0.883	Eosinophil cationic protein. Cytotoxin and helminthotoxin with low-efficiency ribonuclease activity.
RNASE3 - YPV	0.857	
S100A12 - ELA	0.825	S100A12 plays a in the regulation of inflammatory processes and immune response. Its proinflammatory activity involves recruitment of leukocytes, promotion of cytokine and chemokine production, and regulation of leukocyte adhesion and migration.

[a]AUC obtained by univariate ROC curve analysis (Metaboanalyst v4.0). Description based on UniProt protein function description (https://www.uniprot.org/).

envelope precursors such as involucrin, loricrin, small proline-rich proteins, late envelope proteins (LEPs), and filaggrin are cross-linked by transglutaminase forming a 5- to 10 nm mature envelope adjacent to the cell membrane.[90−92] Corneal cell

https://dx.doi.org/10.1021/acs.jproteome.0c00320
J. Proteome Res. 2020, 19, 4496−4515

Figure 9. Summary of the findings provided by clinical data, CImPA/PRM data, and microscopy showing biological events related to gestational ZIKV exposure with and without CZS. Impression cytology membranes collected from a cohort of infants exposed to ZIKV during the first trimester of gestation and with CZS (Zikv^{CZS}) revealed ocular alterations such as optic disc excavation and pallor, abnormal pigment deposition and macular atrophy. These alterations were not detected in the Zikv and Ctrl conditions. The Cellular Imprinting Proteomics approach detected several proteins involved in immune response, cell death, and ocular and neurological disorders differentially regulated. The numbers located close to each bar represent the ratios in each comparison. These molecular alterations were confirmed by microscopy analysis with defects in the morphology of epithelial cells collected from the Zikv^{CZS} group.

envelope bears similarities with the epidermidis.[93] However, the absence of a water-impermeable layer and the need of oxygen and nutrients to permeate the cornea epithelium indicate that envelope proteins are associated with other functions besides protective. Pathological keratinization of the corneal and conjunctival mucosal epithelia is associated with ocular diseases and severe visual loss.[92] Moreover, upregulation of transglutaminase 1, involucrin, filaggrin, and the cytokeratin pair 1/10 proteins was detected in the conjunctiva of patients with chronic cicatricial phase including Stevens-Johnson syndrome, ocular cicatricial pemphigoid and chemical injuries.[94] Keratin 13 (KRT13) was found within the most abundant proteins in the ocular conjunctiva proteome. The data confirmed previous transcriptomic analysis of the human cornea and conjunctiva.[95] KRT13 is an acidic keratin expressed in unkeratinized, stratified squamous epithelium.[96] This protein has been identified as a

https://dx.doi.org/10.1021/acs.jproteome.0c00320
J. Proteome Res. 2020, 19, 4496−4515

specific conjunctival, noncorneal epithelial cell marker using immunocytochemistry applied to impression cytology specimens.[97] Moreover, KRT4/KRT13 pair has been used to identify differentiating cells in internal stratified epithelial cells.[98] The higher expression of KRT13 in Zikv and Zikv^{CZS} compared to control can be associated with keratinization of conjunctival epithelial cells. Taken together, various keratinization-related proteins were regulated in the comparison between Zikv^{CZS} and Zikv with Ctrl. The molecular alterations observed on the ocular surface of infants with CZS were validated by clinical and microscopy analysis. Indeed, the three infants with CZS presented optic disc pallor and excavation and altered macular pigment with pigment deposition. Moreover, bright field microscopy data indicated a higher degree of moderate to severe keratinized ocular epithelial cells in the Zikv^{CZS} compared to control condition (Figure 8E).

Clinical cases of adults infected by ZIKV presenting ocular abnormalities have been described.[99] These data indicate that the neurotropism of the virus is not a necessary factor to elicit ocular dysfunctions. The comparison between Zikv and Ctrl conditions revealed 166 differentially modulated proteins associated with pathways previously described for the Zikv^{CZS} group (Table S2). Interestingly, the fold changes observed for the Zikv vs Ctrl group were lower indicating a mild but significant remodeling of the ocular proteome in infants exposed to ZIKV during gestation. In particular, IFIT3 and IFIH1 were upregulated in the Zikv conditions compared to control. IFIH1 gene encodes a cytoplasmic receptor of the pattern-recognition receptors family that recognizes viral RNA, playing a role in the innate immune response against viral infection.[100,101] The recognition of viral RNA is an ATP-dependent process that induces IFIH1 polymerization and activation of type 1 interferon signaling cascade.[102] IFIH1 loss-of-function variants are unable to produce IFN-β and have been reported to restrict the replication of human respiratory syncytial virus and rhinoviruses.[103]

Congenital Zika syndrome is associated with a wide spectrum of abnormalities that range from mild to severe symptoms.[104] The range of nonmicrocephalic anomalies associated with ZIKV infection poses an important clinical and social challenge. These differences can be attributed to the viral strains and load, time of the infection, and the different genetic background of the hosts. Because of that, these parameters should be considered to get a deeper understanding of this disease. Another important aspect of ocular pathologies in congenital ZIKV infection will be the discordant clinical outcomes in twin pregnancies.[105] Indeed, studying ocular abnormalities in twins with congenital ZIKV infection should help elucidate the mechanism of ZIKV eye infection. The identification of early molecular alterations can improve our understanding of these effects and help in predicting clinical outcomes.[106] Taken together, these results call for an active surveillance of ophthalmological complications in children exposed to ZIKV during the first trimester of gestation but without CZS.

CONCLUSIONS

The CImPA method that is present here is a simple and effective method for the molecular profiling of ocular surface cells. Each eye impression provided as little as 8 μg of starting material to build the first human conjunctival ocular proteome, which is presented here with more than 2000 unique quantifiable proteins. In this study, the method was applied to understand the molecular alterations in children exposed to ZIKV infection during gestation with and without CZS (summarized in Figure 9). The data presented here show a regulation of neutrophil degranulation and immune cells infiltration, neurodevelopment and ocular dysfunctions. Our study using the CImPA indicates the occurrence of neutrophil and eosinophil infiltration and degranulation in the conjunctival epithelium in children exposed to ZIKV infection. The combination of molecular markers and microscopic evaluation of neutrophils could improve the diagnostic and prognostic of ocular dysfunctions in ZIKV infected children. However, additional evidence is needed to clarify the pathophysiological role and clinical relevance of neutrophils in this disease. The "ocular fingerprint" would be a powerful tool, guiding physicians toward a clinical decision on the better treatment aimed at a personalized medicine approach for CZS. Indeed, early diagnosis in children exposed to ZIKV without clinical signs would enable the administration of therapies to control the progression of ocular dysfunctions.

Beyond CZS, the CImPA has the potential to provide detailed molecular data when applied to stroke, multiple sclerosis, Parkinson's, Alzheimer's diseases, and other neurological diseases that involve ocular dysfunction.[107−109] The availability of the advance of large-scale and high-throughput technology will enable the CImPA to be applicable to screen large cohorts. Few biomarker studies applied to human tears have gone from the discovery to the validation phase, and none of them have gone into the clinic.[110] It is urgent to develop standard operating procedures for assessing specific biomarkers using the CImPA method and validate them in multicenter clinical studies.[111,112]

ASSOCIATED CONTENT

Supporting Information

The Supporting Information is available free of charge at https://pubs.acs.org/doi/10.1021/acs.jproteome.0c00320.

Supporting Figures S1 and S2. Figure S1: Comparison of proteins identified from impression cytology membranes using the CImPA. Figure S2: Molecular pathways enriched using the differentially regulated proteins (PDF)

Table S1: List of information for the membranes collected for the CImPA proteomic assay. Table S2: List of peptide ions targeted for validation. Table S3: proteins identified and quantified in the total samples. Table S4: proteins differentially regulated in the ZikvCZS vs Ctrl comparison. Table S5: proteins differentially regulated in the Zikv vs Ctrl comparison. Table S6: proteins differentially regulated in the Zikv^{CZS} vs Zikv comparison. Table S7: validation of differentially expressed proteins by PRM analysis (XLSX)

AUTHOR INFORMATION

Corresponding Authors

Giuseppe Palmisano − *GlycoProteomics Laboratory, Department of Parasitology, Institute of Biomedical Sciences, University of Sao Paulo, Sao Paulo, Brazil;* orcid.org/0000-0003-1336-6151; Email: palmisano.gp@gmail.com

Livia Rosa-Fernandes − *GlycoProteomics Laboratory, Department of Parasitology, Institute of Biomedical Sciences, University of Sao Paulo, Sao Paulo, Brazil; Department of Biochemistry and Molecular Biology, University of Southern Denmark, Odense, Denmark;* orcid.org/0000-0003-1612-1950; Email: liviarosa.f@gmail.com

https://dx.doi.org/10.1021/acs.jproteome.0c00320
J. Proteome Res. 2020, 19, 4496−4515

Authors

Raquel Hora Barbosa − *GlycoProteomics Laboratory, Department of Parasitology, Institute of Biomedical Sciences, University of Sao Paulo, Sao Paulo, Brazil; Molecular and Integrative Physiological Sciences Program, Department of Environmental Health, Harvard School of Public Health, Boston, Massachusetts, United States; Maternal and Child Department, Faculty of Medicine, Fluminense Federal University, Rio de Janeiro, Brazil; Genetics Program, National Cancer Institute, Rio de Janeiro, Brazil*

Maria Luiza B. dos Santos − *Maternal and Child Department, Faculty of Medicine, Fluminense Federal University, Rio de Janeiro, Brazil*

Claudia B. Angeli − *GlycoProteomics Laboratory, Department of Parasitology, Institute of Biomedical Sciences, University of Sao Paulo, Sao Paulo, Brazil*

Thiago P. Silva − *Laboratory of Cellular Biology, Department of Biology, Federal University of Juiz de Fora, Juiz de Fora, Minas Gerais, Brazil*

Rossana C. N. Melo − *Laboratory of Cellular Biology, Department of Biology, Federal University of Juiz de Fora, Juiz de Fora, Minas Gerais, Brazil*

Gilberto Santos de Oliveira − *GlycoProteomics Laboratory, Department of Parasitology, Institute of Biomedical Sciences, University of Sao Paulo, Sao Paulo, Brazil*

Bernardo Lemos − *Molecular and Integrative Physiological Sciences Program, Department of Environmental Health, Harvard School of Public Health, Boston, Massachusetts, United States*

Jennifer E Van Eyk − *Advanced Clinical BioSystems Research Institute, Cedars Sinai Precision Biomarker Laboratories, Barbra Streisand Women's Heart Center, Cedars-Sinai Medical Center, Los Angeles, California, United States;* orcid.org/0000-0001-9050-148X

Martin R. Larsen − *Department of Biochemistry and Molecular Biology, University of Southern Denmark, Odense, Denmark*

Claudete Araújo Cardoso − *Maternal and Child Department, Faculty of Medicine, Fluminense Federal University, Rio de Janeiro, Brazil*

Complete contact information is available at: https://pubs.acs.org/10.1021/acs.jproteome.0c00320

Author Contributions

L.R.-F., R.H.B., and G.P. designed the experiments and performed CImPA sample preparation. L.R.-F. and G.P. performed analytical method development, mass spectrometry analysis, data interpretation, P.R.M. analyzed and wrote the manuscript. R.H.B. collected the impression cytology membranes and respective informed and written consents. C.A.C. performed the cohort selection and coordinates the clinical follow-up study. M.L.B.S., C.B.A., and G.S.O. assisted on CImPA sample preparation. B.L. assisted in the experimental design. J.E.V. assisted on data interpretation and revision of the manuscript. M.R.L. assisted on analytical method development, mass spectrometry analysis, and revision of the manuscript. T.P.S. and R.C.M. performed microscopy analyses. All authors contributed in editing the manuscript and approved the final version.

Author Contributions

◆L.R.-F. and R.H.B. share first authorship.

Notes

The authors declare no competing financial interest.

Data availability: The mass spectrometry-based proteomics data have been deposited to the ProteomeXchange Consortium under accession PXD014038.

■ ACKNOWLEDGMENTS

R.H.B. was supported by FAPERJ (201.779/2017), G.P. was supported by FAPESP (2014/06863-3, 2018/18257-1, 2018/15549-1), and CNPq ("Bolsa de Produtividade"), MLBS was supported by CAPES (Finance Code 001), R.C.M. was supported by CNPq (434914/2018-5 and 309734/2018-5). This work was also supported by the VILLUM Center for Bioanalytical Sciences at the University of Southern Denmark. The authors thank children and their families that participated in the study, Unidade de Pesquisa Clínica/UPC, and Zika Collaborative Group/UFF.

■ REFERENCES

(1) Lee, C. Y.; Ng, L. F. P. Zika virus: from an obscurity to a priority. *Microbes Infect.* **2018**, *20* (11−12), 635−645.

(2) Dick, G. W.; Kitchen, S. F.; Haddow, A. J. Zika virus. I. Isolations and serological specificity. *Trans. R. Soc. Trop. Med. Hyg.* **1952**, *46* (5), 509−20.

(3) Posen, H. J.; Keystone, J. S.; Gubbay, J. B.; Morris, S. K. Epidemiology of Zika virus, 1947−2007. *BMJ. global health* **2016**, *1* (2), e000087.

(4) Lanciotti, R. S.; Kosoy, O. L.; Laven, J. J.; Velez, J. O.; Lambert, A. J.; Johnson, A. J.; Stanfield, S. M.; Duffy, M. R. Genetic and serologic properties of Zika virus associated with an epidemic, Yap State, Micronesia, 2007. *Emerging Infect. Dis.* **2008**, *14* (8), 1232−9.

(5) de Araujo, T. V. B.; Ximenes, R. A. A.; Miranda-Filho, D. B.; Souza, W. V.; Montarroyos, U. R.; de Melo, A. P. L.; Valongueiro, S.; de Albuquerque, M.; Braga, C.; Filho, S. P. B.; Cordeiro, M. T.; Vazquez, E.; Cruz, D.; Henriques, C. M. P.; Bezerra, L. C. A.; Castanha, P.; Dhalia, R.; Marques-Junior, E. T. A.; Martelli, C. M. T.; Rodrigues, L. C. Association between microcephaly, Zika virus infection, and other risk factors in Brazil: final report of a case-control study. *Lancet Infect. Dis.* **2018**, *18* (3), 328−336.

(6) Soares de Oliveira-Szejnfeld, P.; Levine, D.; Melo, A. S.; Amorim, M. M.; Batista, A. G.; Chimelli, L.; Tanuri, A.; Aguiar, R. S.; Malinger, G.; Ximenes, R.; Robertson, R.; Szejnfeld, J.; Tovar-Moll, F. Congenital Brain Abnormalities and Zika Virus: What the Radiologist Can Expect to See Prenatally and Postnatally. *Radiology* **2016**, *281* (1), 203−18.

(7) Moore, C. A.; Staples, J. E.; Dobyns, W. B.; Pessoa, A.; Ventura, C. V.; Fonseca, E. B.; Ribeiro, E. M.; Ventura, L. O.; Neto, N. N.; Arena, J. F.; Rasmussen, S. A. Characterizing the Pattern of Anomalies in Congenital Zika Syndrome for Pediatric Clinicians. *JAMA pediatrics* **2017**, *171* (3), 288−295.

(8) Sahiner, F.; Sig, A. K.; Savasci, U.; Tekin, K.; Akay, F. Zika Virus-associated Ocular and Neurologic Disorders: The Emergence of New Evidence. *Pediatric infectious disease journal* **2017**, *36* (12), e341−e346.

(9) de Paula Freitas, B.; de Oliveira Dias, J. R.; Prazeres, J.; Sacramento, G. A.; Ko, A. I.; Maia, M.; Belfort, R., Jr. Ocular Findings in Infants With Microcephaly Associated With Presumed Zika Virus Congenital Infection in Salvador, Brazil. *JAMA ophthalmology* **2016**, *134* (5), 529−535.

(10) Miranda, H. A., 2nd; Costa, M. C.; Frazao, M. A. M.; Simao, N.; Franchischini, S.; Moshfeghi, D. M. Expanded Spectrum of Congenital Ocular Findings in Microcephaly with Presumed Zika Infection. *Ophthalmology* **2016**, *123* (8), 1788−1794.

(11) de Oliveira Dias, J. R.; Ventura, C. V.; Borba, P. D.; de Paula Freitas, B.; Pierroti, L. C.; do Nascimento, A. P.; de Moraes, N. S. B.; Maia, M.; Belfort, R., Jr. Infants with Congenital Zika Syndrome and Ocular Findings from Sao Paulo, Brazil: Spread of Infection. *Retinal Cases & Brief Rep.* **2018**, *12* (4), 382−386.

(12) Ventura, C. V.; Maia, M.; Bravo-Filho, V.; Gois, A. L.; Belfort, R., Jr. Zika virus in Brazil and macular atrophy in a child with microcephaly. *Lancet* **2016**, *387* (10015), 228.
(13) Ventura, C. V.; Ventura, L. O.; Bravo-Filho, V.; Martins, T. T.; Berrocal, A. M.; Gois, A. L.; de Oliveira Dias, J. R.; Araujo, L.; Escariao, P.; van der Linden, V.; Belfort, R., Jr.; Maia, M. Optical Coherence Tomography of Retinal Lesions in Infants With Congenital Zika Syndrome. *JAMA ophthalmology* **2016**, *134* (12), 1420−1427.
(14) Guevara, J. G.; Agarwal-Sinha, S. Ocular abnormalities in congenital Zika syndrome: a case report, and review of the literature. *J. Med. Case Rep.* **2018**, *12* (1), 161.
(15) van der Linden, V.; Pessoa, A.; Dobyns, W.; Barkovich, A. J.; Junior, H. V.; Filho, E. L.; Ribeiro, E. M.; Leal, M. C.; Coimbra, P. P.; Aragao, M. F.; Vercosa, I.; Ventura, C.; Ramos, R. C.; Cruz, D. D.; Cordeiro, M. T.; Mota, V. M.; Dott, M.; Hillard, C.; Moore, C. A. , Description of 13 Infants Born During October 2015-January 2016 With Congenital Zika Virus Infection Without Microcephaly at Birth - Brazil. *MMWR Morb Mortal Wkly Rep* **2016**, *65* (47), 1343−1348.
(16) Stockwell, S. The CDC Updates Guidelines for Congenital Zika. *Am. J. Nurs.* **2018**, *118* (5), 14.
(17) London, A.; Benhar, I.; Schwartz, M. The retina as a window to the brain-from eye research to CNS disorders. *Nat. Rev. Neurol.* **2013**, *9* (1), 44−53.
(18) Wong, T. Y.; Klein, R.; Sharrett, A. R.; Couper, D. J.; Klein, B. E.; Liao, D. P.; Hubbard, L. D.; Mosley, T. H.; Study, A. I. A. R. i. C. Cerebral white matter lesions, retinopathy, and incident clinical stroke. *JAMA* **2002**, *288* (1), 67−74.
(19) Fisher, J. B.; Jacobs, D. A.; Markowitz, C. E.; Galetta, S. L.; Volpe, N. J.; Nano-Schiavi, M. L.; Baier, M. L.; Frohman, E. M.; Winslow, H.; Frohman, T. C.; Calabresi, P. A.; Maguire, M. G.; Cutter, G. R.; Balcer, L. J. Relation of visual function to retinal nerve fiber layer thickness in multiple sclerosis. *Ophthalmology* **2006**, *113* (2), 324−32.
(20) Moschos, M. M.; Tagaris, G.; Markopoulos, I.; Margetis, I.; Tsapakis, S.; Kanakis, M.; Koutsandrea, C. Morphologic changes and functional retinal impairment in patients with Parkinson disease without visual loss. *European journal of ophthalmology* **2011**, *21* (1), 24−9.
(21) Goldstein, L. E.; Muffat, J. A.; Cherny, R. A.; Moir, R. D.; Ericsson, M. H.; Huang, X.; Mavros, C.; Coccia, J. A.; Faget, K. Y.; Fitch, K. A.; Masters, C. L.; Tanzi, R. E.; Chylack, L. T., Jr.; Bush, A. I. Cytosolic beta-amyloid deposition and supranuclear cataracts in lenses from people with Alzheimer's disease. *Lancet* **2003**, *361* (9365), 1258−65.
(22) de Paula Freitas, B.; Ventura, C. V.; Maia, M.; Belfort, R., Jr. Zika virus and the eye. *Current opinion in ophthalmology* **2017**, *28* (6), 595−599.
(23) de Paula Freitas, B.; Zin, A.; Ko, A.; Maia, M.; Ventura, C. V.; Belfort, R., Jr. Anterior-Segment Ocular Findings and Microphthalmia in Congenital Zika Syndrome. *Ophthalmology* **2017**, *124* (12), 1876−1878.
(24) Fernandez, M. P.; Parra Saad, E.; Ospina Martinez, M.; Corchuelo, S.; Mercado Reyes, M.; Herrera, M. J.; Parra Saavedra, M.; Rico, A.; Fernandez, A. M.; Lee, R. K.; Ventura, C. V.; Berrocal, A. M.; Dubovy, S. R. Ocular Histopathologic Features of Congenital Zika Syndrome. *JAMA ophthalmology* **2017**, *135* (11), 1163−1169.
(25) Ritter, J. M.; Martines, R. B.; Zaki, S. R. Zika Virus: Pathology From the Pandemic. *Arch. Pathol. Lab. Med.* **2017**, *141* (1), 49−59.
(26) Ventura, C. V.; Maia, M.; Travassos, S. B.; Martins, T. T.; Patriota, F.; Nunes, M. E.; Agra, C.; Torres, V. L.; van der Linden, V.; Ramos, R. C.; Rocha, M. A.; Silva, P. S.; Ventura, L. O.; Belfort, R., Jr. Risk Factors Associated With the Ophthalmoscopic Findings Identified in Infants With Presumed Zika Virus Congenital Infection. *JAMA ophthalmology* **2016**, *134* (8), 912−8.
(27) Zin, A. A.; Tsui, I.; Rossetto, J.; Vasconcelos, Z.; Adachi, K.; Valderramos, S.; Halai, U. A.; Pone, M.; Pone, S. M.; Silveira Filho, J. C. B.; Aibe, M. S.; da Costa, A. C. C.; Zin, O. A.; Belfort, R., Jr.; Brasil, P.; Nielsen-Saines, K.; Moreira, M. E. L. Screening Criteria for Ophthalmic Manifestations of Congenital Zika Virus Infection. *JAMA pediatrics* **2017**, *171* (9), 847−854.
(28) Valentine, G.; Marquez, L.; Pammi, M. Zika Virus-Associated Microcephaly and Eye Lesions in the Newborn. *Journal of the Pediatric Infectious Diseases Society* **2016**, *5* (3), 323−8.
(29) Ventura, C. V.; Maia, M.; Dias, N.; Ventura, L. O.; Belfort, R., Jr. Zika: neurological and ocular findings in infant without microcephaly. *Lancet* **2016**, *387* (10037), 2502.
(30) Vianna, R. A. O.; Lovero, K. L.; Oliveira, S. A.; Fernandes, A. R.; Santos, T.; Lima, L.; Carvalho, F. R.; Quintans, M. D. S.; Bueno, A. C.; Torbey, A. F. M.; Souza, A.; Farias, A. O. P.; Camacho, L. A. B.; Riley, L. W.; Cardoso, C. A. A. Children Born to Mothers with Rash During Zika Virus Epidemic in Brazil: First 18 Months of Life. *J. Trop Pediatr* **2019**, *65*, 592.
(31) Barbosa, R. H.; dos Santos, M. L. B.; Silva, T. P.; Rosa-Fernandes, L.; Pinto, A.; Spínola, P. S.; Bonvicino, C. R.; Fernandes, P. V.; Evandro Lucena, E.; Giuseppe Palmisano, G.; Melo, R. C. N.; Cardoso, C.; Lemos, B. Impression cytology is a non-invasive and effective method for ocular cell obtention from babies with Congenital Zika Syndrome: perspectives in OMIC studies. *BioRxiv* **2019**.
(32) Kawahara, R.; Rosa-Fernandes, L.; Dos Santos, A. F.; Bandeira, C. L.; Dombrowski, J. G.; Souza, R. M.; Da Fonseca, M. P.; Festuccia, W. T.; Labriola, L.; Larsen, M. R.; Marinho, C. R. F.; Palmisano, G. Integrated Proteomics Reveals Apoptosis-related Mechanisms Associated with Placental Malaria. *Mol. Cell. Proteomics* **2019**, *18* (2), 182−199.
(33) Gobom, J.; Nordhoff, E.; Mirgorodskaya, E.; Ekman, R.; Roepstorff, P. Sample purification and preparation technique based on nano-scale reversed-phase columns for the sensitive analysis of complex peptide mixtures by matrix-assisted laser desorption/ionization mass spectrometry. *J. Mass Spectrom.* **1999**, *34* (2), 105−16.
(34) Rosa-Fernandes, L.; Cugola, F. R.; Russo, F. B.; Kawahara, R.; de Melo Freire, C. C.; Leite, P. E. C.; Bassi Stern, A. C.; Angeli, C. B.; de Oliveira, D. B. L.; Melo, S. R.; Zanotto, P. M. A.; Durigon, E. L.; Larsen, M. R.; Beltrao-Braga, P. C. B.; Palmisano, G. Zika Virus Impairs Neurogenesis and Synaptogenesis Pathways in Human Neural Stem Cells and Neurons. *Front. Cell. Neurosci.* **2019**, *13*, 64.
(35) Navarro, P.; Trevisan-Herraz, M.; Bonzon-Kulichenko, E.; Nunez, E.; Martinez-Acedo, P.; Perez-Hernandez, D.; Jorge, I.; Mesa, R.; Calvo, E.; Carrascal, M.; Hernaez, M. L.; Garcia, F.; Barcena, J. A.; Ashman, K.; Abian, J.; Gil, C.; Redondo, J. M.; Vazquez, J. General statistical framework for quantitative proteomics by stable isotope labeling. *J. Proteome Res.* **2014**, *13* (3), 1234−47.
(36) Ahmad, M. T.; Zhang, P.; Dufresne, C.; Ferrucci, L.; Semba, R. D. The Human Eye Proteome Project: Updates on an Emerging Proteome. *Proteomics* **2018**, *18* (5−6), 1700394.
(37) Wistow, G.; Peterson, K.; Gao, J.; Buchoff, P.; Jaworski, C.; Bowes-Rickman, C.; Ebright, J. N.; Hauser, M. A.; Hoover, D. NEIBank: genomics and bioinformatics resources for vision research. *Mol. Vis.* **2008**, *14*, 1327−37.
(38) Uhlen, M.; Fagerberg, L.; Hallstrom, B. M.; Lindskog, C.; Oksvold, P.; Mardinoglu, A.; Sivertsson, A.; Kampf, C.; Sjostedt, E.; Asplund, A.; Olsson, I.; Edlund, K.; Lundberg, E.; Navani, S.; Szigyarto, C. A.; Odeberg, J.; Djureinovic, D.; Takanen, J. O.; Hober, S.; Alm, T.; Edqvist, P. H.; Berling, H.; Tegel, H.; Mulder, J.; Rockberg, J.; Nilsson, P.; Schwenk, J. M.; Hamsten, M.; von Feilitzen, K.; Forsberg, M.; Persson, L.; Johansson, F.; Zwahlen, M.; von Heijne, G.; Nielsen, J.; Ponten, F. Proteomics. Tissue-based map of the human proteome. *Science* **2015**, *347* (6220), 1260419.
(39) Schwenk, J. M.; Omenn, G. S.; Sun, Z.; Campbell, D. S.; Baker, M. S.; Overall, C. M.; Aebersold, R.; Moritz, R. L.; Deutsch, E. W. The Human Plasma Proteome Draft of 2017: Building on the Human Plasma PeptideAtlas from Mass Spectrometry and Complementary Assays. *J. Proteome Res.* **2017**, *16* (12), 4299−4310.
(40) Citirik, M.; Berker, N.; Haksever, H.; Elgin, U.; Ustun, H. Conjunctival impression cytology in non-proliferative and proliferative diabetic retinopathy. *Int. J. Ophthalmol.* **2014**, *7* (2), 321−325.
(41) Uzel, M. M.; Citirik, M.; Kekilli, M.; Cicek, P. Local ocular surface parameters in patients with systemic celiac disease. *Eye (London, U. K.)* **2017**, *31* (7), 1093−1098.

https://dx.doi.org/10.1021/acs.jproteome.0c00320
J. Proteome Res. 2020, 19, 4496−4515

(42) Mrugacz, M.; Zak, J.; Bakunowicz-Lazarczyk, A.; Wysocka, J.; Minarowska, A. Flow cytometric analysis of HLA-DR antigen in conjunctival epithelial cells of patients with cystic fibrosis. *Eye (London, U. K.)* **2007**, *21* (8), 1062−6.
(43) Soria, J.; Acera, A.; Duran, J. A.; Boto-de-Los-Bueis, A.; Del-Hierro-Zarzuelo, A.; Gonzalez, N.; Reigada, R.; Suarez, T. The analysis of human conjunctival epithelium proteome in ocular surface diseases using impression cytology and 2D-DIGE. *Exp. Eye Res.* **2018**, *167*, 31−43.
(44) Glasgow, B. J.; Abduragimov, A. R.; Farahbakhsh, Z. T.; Faull, K. F.; Hubbell, W. L. Tear lipocalins bind a broad array of lipid ligands. *Curr. Eye Res.* **1995**, *14* (5), 363−72.
(45) Elangovan, N.; Lee, Y. C.; Tzeng, W. F.; Chu, S. T. Delivery of ferric ion to mouse spermatozoa is mediated by lipocalin internalization. *Biochem. Biophys. Res. Commun.* **2004**, *319* (4), 1096−104.
(46) Kjeldsen, L.; Cowland, J. B.; Borregaard, N. Human neutrophil gelatinase-associated lipocalin and homologous proteins in rat and mouse. *Biochim. Biophys. Acta, Protein Struct. Mol. Enzymol.* **2000**, *1482* (1−2), 272−83.
(47) Flo, T. H.; Smith, K. D.; Sato, S.; Rodriguez, D. J.; Holmes, M. A.; Strong, R. K.; Akira, S.; Aderem, A. Lipocalin 2 mediates an innate immune response to bacterial infection by sequestrating iron. *Nature* **2004**, *432* (7019), 917−21.
(48) Moschen, A. R.; Adolph, T. E.; Gerner, R. R.; Wieser, V.; Tilg, H. Lipocalin-2: A Master Mediator of Intestinal and Metabolic Inflammation. *Trends Endocrinol. Metab.* **2017**, *28* (5), 388−397.
(49) Dota, A.; Nishida, K.; Adachi, W.; Nakamura, T.; Koizumi, N.; Kawamoto, S.; Okubo, K.; Kinoshita, S. An expression profile of active genes in human conjunctival epithelium. *Exp. Eye Res.* **2001**, *72* (3), 235−41.
(50) Thiel, M. A.; Bossart, W.; Bernauer, W. Improved impression cytology techniques for the immunopathological diagnosis of superficial viral infections. *Br. J. Ophthalmol.* **1997**, *81* (11), 984−8.
(51) Sun, J.; Wu, D.; Zhong, H.; Guan, D.; Zhang, H.; Tan, Q.; Ke, C. Presence of Zika Virus in Conjunctival Fluid. *JAMA Ophthalmol.* **2016**, *134* (11), 1330−1332.
(52) Bai, F.; Kong, K. F.; Dai, J.; Qian, F.; Zhang, L.; Brown, C. R.; Fikrig, E.; Montgomery, R. R. A paradoxical role for neutrophils in the pathogenesis of West Nile virus. *J. Infect. Dis.* **2010**, *202* (12), 1804−12.
(53) Srivastava, S.; Khanna, N.; Saxena, S. K.; Singh, A.; Mathur, A.; Dhole, T. N. Degradation of Japanese encephalitis virus by neutrophils. *Int. J. Exp. Pathol.* **1999**, *80* (1), 17−24.
(54) Jarczak, J.; Kosciuczuk, E. M.; Lisowski, P.; Strzalkowska, N.; Jozwik, A.; Horbanczuk, J.; Krzyzewski, J.; Zwierzchowski, L.; Bagnicka, E. Defensins: natural component of human innate immunity. *Hum. Immunol.* **2013**, *74* (9), 1069−79.
(55) Daher, K. A.; Selsted, M. E.; Lehrer, R. I. Direct inactivation of viruses by human granulocyte defensins. *J. Virol.* **1986**, *60* (3), 1068−74.
(56) Fraisier, C.; Papa, A.; Granjeaud, S.; Hintzen, R.; Martina, B.; Camoin, L.; Almeras, L. Cerebrospinal fluid biomarker candidates associated with human WNV neuroinvasive disease. *PLoS One* **2014**, *9* (4), e93637.
(57) Loke, P.; Hammond, S. N.; Leung, J. M.; Kim, C. C.; Batra, S.; Rocha, C.; Balmaseda, A.; Harris, E. Gene expression patterns of dengue virus-infected children from nicaragua reveal a distinct signature of increased metabolism. *PLoS Neglected Trop. Dis.* **2010**, *4* (6), e710.
(58) Amaral, D. C.; Rachid, M. A.; Vilela, M. C.; Campos, R. D.; Ferreira, G. P.; Rodrigues, D. H.; Lacerda-Queiroz, N.; Miranda, A. S.; Costa, V. V.; Campos, M. A.; Kroon, E. G.; Teixeira, M. M.; Teixeira, A. L. Intracerebral infection with dengue-3 virus induces meningoencephalitis and behavioral changes that precede lethality in mice. *J. Neuroinflammation* **2011**, *8*, 23.
(59) Ubol, S.; Masrinoul, P.; Chaijaruwanich, J.; Kalayanarooj, S.; Charoensirisuthikul, T.; Kasisith, J. Differences in global gene expression in peripheral blood mononuclear cells indicate a significant role of the innate responses in progression of dengue fever but not dengue hemorrhagic fever. *J. Infect. Dis.* **2008**, *197* (10), 1459−67.
(60) Jampol, L. M.; Ferris, F. L., 3rd; Bishop, R. J. Ebola and the eye. *JAMA ophthalmology* **2015**, *133* (10), 1105−6.
(61) Yahia, S. B.; Khairallah, M. Ocular manifestations of West Nile virus infection. *Int. J. Med. Sci.* **2009**, *6* (3), 114−5.
(62) Manangeeswaran, M.; Kielczewski, J. L.; Sen, H. N.; Xu, B. C.; Ireland, D. D. C.; McWilliams, I. L.; Chan, C. C.; Caspi, R. R.; Verthelyi, D. ZIKA virus infection causes persistent chorioretinal lesions. *Emerging Microbes Infect.* **2018**, *7* (1), 1−15.
(63) Kodati, S.; Palmore, T. N.; Spellman, F. A.; Cunningham, D.; Weistrop, B.; Sen, H. N. Bilateral posterior uveitis associated with Zika virus infection. *Lancet* **2017**, *389* (10064), 125−126.
(64) Ventura, C. V.; Maia, M.; Ventura, B. V.; Linden, V. V.; Araujo, E. B.; Ramos, R. C.; Rocha, M. A.; Carvalho, M. D.; Belfort, R., Jr.; Ventura, L. O. Ophthalmological findings in infants with microcephaly and presumable intra-uterus Zika virus infection. *Arq Bras Oftalmol* **2016**, *79* (1), 1−3.
(65) Lalitha, P.; Rathinam, S.; Banushree, K.; Maheshkumar, S.; Vijayakumar, R.; Sathe, P. Ocular involvement associated with an epidemic outbreak of chikungunya virus infection. *Am. J. Ophthalmol.* **2007**, *144* (4), 552−6.
(66) Chanana, B.; Azad, R. V.; Nair, S. Bilateral macular choroiditis following Chikungunya virus infection. *Eye (London, U. K.)* **2007**, *21* (7), 1020−1.
(67) Perez, V. L.; Caspi, R. R. Immune mechanisms in inflammatory and degenerative eye disease. *Trends Immunol.* **2015**, *36* (6), 354−63.
(68) Wang, W.; Li, G.; Wu, D.; Luo, Z.; Pan, P.; Tian, M.; Wang, Y.; Xiao, F.; Li, A.; Wu, K.; Liu, X.; Rao, L.; Liu, F.; Liu, Y.; Wu, J. Zika virus infection induces host inflammatory responses by facilitating NLRP3 inflammasome assembly and interleukin-1beta secretion. *Nat. Commun.* **2018**, *9* (1), 106.
(69) Williams, G. P.; Nightingale, P.; Southworth, S.; Denniston, A. K.; Tomlins, P. J.; Turner, S.; Hamburger, J.; Bowman, S. J.; Curnow, S. J.; Rauz, S. Conjunctival Neutrophils Predict Progressive Scarring in Ocular Mucous Membrane Pemphigoid. *Invest. Ophthalmol. Visual Sci.* **2016**, *57* (13), 5457−5469.
(70) Williams, G. P.; Tomlins, P. J.; Denniston, A. K.; Southworth, H. S.; Sreekantham, S.; Curnow, S. J.; Rauz, S. Elevation of conjunctival epithelial CD45INTCD11b(+)CD16(+)CD14(−) neutrophils in ocular Stevens-Johnson syndrome and toxic epidermal necrolysis. *Invest. Ophthalmol. Visual Sci.* **2013**, *54* (7), 4578−85.
(71) Heiligenhaus, A.; Schaller, J.; Mauss, S.; Engelbrecht, S.; Dutt, J. E.; Foster, C. S.; Steuhl, K. P. Eosinophil granule proteins expressed in ocular cicatricial pemphigoid. *Br. J. Ophthalmol.* **1998**, *82* (3), 312−7.
(72) Trocme, S. D.; Bartley, G. B.; Campbell, R. J.; Gleich, G. J.; Leiferman, K. M. Eosinophil and neutrophil degranulation in ophthalmic lesions of Wegener's granulomatosis. *Arch. Ophthalmol.* **1991**, *109* (11), 1585−9.
(73) Gao, J.; Cui, J. Z.; To, E.; Cao, S.; Matsubara, J. A. Evidence for the activation of pyroptotic and apoptotic pathways in RPE cells associated with NLRP3 inflammasome in the rodent eye. *J. Neuroinflammation* **2018**, *15* (1), 15.
(74) Sun, N.; Zhang, H., Pyroptosis in pterygium pathogenesis. *Biosci. Rep.* **2018**, *38* (3). DOI: 10.1042/BSR20180282
(75) Wald, G. Molecular basis of visual excitation. *Science* **1968**, *162* (3850), 230−9.
(76) Janecke, A. R.; Thompson, D. A.; Utermann, G.; Becker, C.; Hubner, C. A.; Schmid, E.; McHenry, C. L.; Nair, A. R.; Ruschendorf, F.; Heckenlively, J.; Wissinger, B.; Nurnberg, P.; Gal, A. Mutations in RDH12 encoding a photoreceptor cell retinol dehydrogenase cause childhood-onset severe retinal dystrophy. *Nat. Genet.* **2004**, *36* (8), 850−4.
(77) Gu, S. M.; Thompson, D. A.; Srikumari, C. R.; Lorenz, B.; Finckh, U.; Nicoletti, A.; Murthy, K. R.; Rathmann, M.; Kumaramanickavel, G.; Denton, M. J.; Gal, A. Mutations in RPE65 cause autosomal recessive childhood-onset severe retinal dystrophy. *Nat. Genet.* **1997**, *17* (2), 194−7.
(78) Allikmets, R.; Singh, N.; Sun, H.; Shroyer, N. F.; Hutchinson, A.; Chidambaram, A.; Gerrard, B.; Baird, L.; Stauffer, D.; Peiffer, A.; Rattner, A.; Smallwood, P.; Li, Y.; Anderson, K. L.; Lewis, R. A.;

Nathans, J.; Leppert, M.; Dean, M.; Lupski, J. R. A photoreceptor cell-specific ATP-binding transporter gene (ABCR) is mutated in recessive Stargardt macular dystrophy. *Nat. Genet.* **1997**, *15* (3), 236−46.
(79) Stefanovic, Z.; Mijailovic, B.; Arneric, S.; Stefanovic, M.; Mikuska, M. [Immunofluorescent tests in chronic liver diseases]. *Lijec Vjesn* **1975**, *97* (1), 11−5.
(80) Ong, D. E.; Davis, J. T.; O'Day, W. T.; Bok, D. Synthesis and secretion of retinol-binding protein and transthyretin by cultured retinal pigment epithelium. *Biochemistry* **1994**, *33* (7), 1835−42.
(81) Soprano, D. R.; Soprano, K. J.; Goodman, D. S. Retinol-binding protein messenger RNA levels in the liver and in extrahepatic tissues of the rat. *J. Lipid Res.* **1986**, *27* (2), 166−171.
(82) Kanai, M.; Raz, A.; Goodman, D. S. Retinol-binding protein: the transport protein for vitamin A in human plasma. *J. Clin. Invest.* **1968**, *47* (9), 2025−44.
(83) Cukras, C.; Gaasterland, T.; Lee, P.; Gudiseva, H. V.; Chavali, V. R.; Pullakhandam, R.; Maranhao, B.; Edsall, L.; Soares, S.; Reddy, G. B.; Sieving, P. A.; Ayyagari, R. Exome analysis identified a novel mutation in the RBP4 gene in a consanguineous pedigree with retinal dystrophy and developmental abnormalities. *PLoS One* **2012**, *7* (11), e50205.
(84) Seeliger, M. W.; Biesalski, H. K.; Wissinger, B.; Gollnick, H.; Gielen, S.; Frank, J.; Beck, S.; Zrenner, E. Phenotype in retinol deficiency due to a hereditary defect in retinol binding protein synthesis. *Investig. Ophthalmol. Visual Sci.* **1999**, *40* (1), 3−11.
(85) Liu, L.; Suzuki, T.; Shen, J.; Wakana, S.; Araki, K.; Yamamura, K. I.; Lei, L.; Li, Z. Rescue of retinal morphology and function in a humanized mouse at the mouse retinol-binding protein locus. *Lab. Invest.* **2017**, *97* (4), 395−408.
(86) Quadro, L.; Blaner, W. S.; Hamberger, L.; Van Gelder, R. N.; Vogel, S.; Piantedosi, R.; Gouras, P.; Colantuoni, V.; Gottesman, M. E. Muscle expression of human retinol-binding protein (RBP). Suppression of the visual defect of RBP knockout mice. *J. Biol. Chem.* **2002**, *277* (33), 30191−7.
(87) Quadro, L.; Blaner, W. S.; Salchow, D. J.; Vogel, S.; Piantedosi, R.; Gouras, P.; Freeman, S.; Cosma, M. P.; Colantuoni, V.; Gottesman, M. E. Impaired retinal function and vitamin A availability in mice lacking retinol-binding protein. *EMBO J.* **1999**, *18* (17), 4633−44.
(88) Summers, J. A.; Harper, A. R.; Feasley, C. L.; Van-Der-Wel, H.; Byrum, J. N.; Hermann, M.; West, C. M. Identification of Apolipoprotein A-I as a Retinoic Acid-binding Protein in the Eye. *J. Biol. Chem.* **2016**, *291* (36), 18991−9005.
(89) Segre, J. Complex redundancy to build a simple epidermal permeability barrier. *Curr. Opin. Cell Biol.* **2003**, *15* (6), 776−82.
(90) Bernerd, F.; Asselineau, D. Successive alteration and recovery of epidermal differentiation and morphogenesis after specific UVB-damages in skin reconstructed in vitro. *Dev. Biol.* **1997**, *183* (2), 123−38.
(91) Marshall, D.; Hardman, M. J.; Nield, K. M.; Byrne, C. Differentially expressed late constituents of the epidermal cornified envelope. *Proc. Natl. Acad. Sci. U. S. A.* **2001**, *98* (23), 13031−6.
(92) Nakamura, T.; Nishida, K.; Dota, A.; Matsuki, M.; Yamanishi, K.; Kinoshita, S. Elevated expression of transglutaminase 1 and keratinization-related proteins in conjunctiva in severe ocular surface disease. *Investig. ophthalmol. Visual Sci.* **2001**, *42* (3), 549−56.
(93) Castro-Munozledo, F. Development of a spontaneous permanent cell line of rabbit corneal epithelial cells that undergoes sequential stages of differentiation in cell culture. *J. Cell Sci.* **1994**, *107* (Pt 8), 2343−51.
(94) Tong, L.; Corrales, R. M.; Chen, Z.; Villarreal, A. L.; De Paiva, C. S.; Beuerman, R.; Li, D. Q.; Pflugfelder, S. C. Expression and regulation of cornified envelope proteins in human corneal epithelium. *Invest. Ophthalmol. Visual Sci.* **2006**, *47* (5), 1938−46.
(95) Turner, H. C.; Budak, M. T.; Akinci, M. A.; Wolosin, J. M. Comparative analysis of human conjunctival and corneal epithelial gene expression with oligonucleotide microarrays. *Invest. Ophthalmol. Visual Sci.* **2007**, *48* (5), 2050−61.
(96) Waseem, A.; Alam, Y.; Dogan, B.; White, K. N.; Leigh, I. M.; Waseem, N. H. Isolation, sequence and expression of the gene encoding human keratin 13. *Gene* **1998**, *215* (2), 269−79.
(97) Ramirez-Miranda, A.; Nakatsu, M. N.; Zarei-Ghanavati, S.; Nguyen, C. V.; Deng, S. X. Keratin 13 is a more specific marker of conjunctival epithelium than keratin 19. *Mol. Vis.* **2011**, *17*, 1652−61.
(98) Albers, K. M. Keratin biochemistry. *Clin Dermatol* **1996**, *14* (4), 309−20.
(99) Singh, M. S.; Marquezan, M. C.; Omiadze, R.; Reddy, A. K.; Belfort, R., Jr.; May, W. N. Inner retinal vasculopathy in Zika virus disease. *Am. J. Ophthalmol Case Rep* **2018**, *10*, 6−7.
(100) Slater, L.; Bartlett, N. W.; Haas, J. J.; Zhu, J.; Message, S. D.; Walton, R. P.; Sykes, A.; Dahdaleh, S.; Clarke, D. L.; Belvisi, M. G.; Kon, O. M.; Fujita, T.; Jeffery, P. K.; Johnston, S. L.; Edwards, M. R. Co-ordinated role of TLR3, RIG-I and MDA5 in the innate response to rhinovirus in bronchial epithelium. *PLoS Pathog.* **2010**, *6* (11), e1001178.
(101) Gitlin, L.; Barchet, W.; Gilfillan, S.; Cella, M.; Beutler, B.; Flavell, R. A.; Diamond, M. S.; Colonna, M. Essential role of mda-5 in type I IFN responses to polyriboinosinic:polyribocytidylic acid and encephalomyocarditis picornavirus. *Proc. Natl. Acad. Sci. U. S. A.* **2006**, *103* (22), 8459−64.
(102) Loo, Y. M.; Gale, M., Jr. Immune signaling by RIG-I-like receptors. *Immunity* **2011**, *34* (5), 680−92.
(103) Asgari, S.; Schlapbach, L. J.; Anchisi, S.; Hammer, C.; Bartha, I.; Junier, T.; Mottet-Osman, G.; Posfay-Barbe, K. M.; Longchamp, D.; Stocker, M.; Cordey, S.; Kaiser, L.; Riedel, T.; Kenna, T.; Long, D.; Schibler, A.; Telenti, A.; Tapparel, C.; McLaren, P. J.; Garcin, D.; Fellay, J. Severe viral respiratory infections in children with IFIH1 loss-of-function mutations. *Proc. Natl. Acad. Sci. U. S. A.* **2017**, *114* (31), 8342−8347.
(104) Aragao, M.; Holanda, A. C.; Brainer-Lima, A. M.; Petribu, N. C. L.; Castillo, M.; van der Linden, V.; Serpa, S. C.; Tenorio, A. G.; Travassos, P. T. C.; Cordeiro, M. T.; Sarteschi, C.; Valenca, M. M.; Costello, A. Nonmicrocephalic Infants with Congenital Zika Syndrome Suspected Only after Neuroimaging Evaluation Compared with Those with Microcephaly at Birth and Postnatally: How Large Is the Zika Virus "Iceberg"? *AJNR Am. J. Neuroradiol* **2017**, *38* (7), 1427−1434.
(105) Linden, V. V.; Linden, H. V. J.; Leal, M. C.; Rolim, E. L. F.; Linden, A. V.; Aragao, M.; Brainer-Lima, A. M.; Cruz, D.; Ventura, L. O.; Florencio, T. L. T.; Cordeiro, M. T.; Caudas, S. D. S. N.; Ramos, R. C. Discordant clinical outcomes of congenital Zika virus infection in twin pregnancies. *Arq. Neuro-Psiquiatr.* **2017**, *75* (6), 381−386.
(106) Walker, C. L.; Little, M. E.; Roby, J. A.; Armistead, B.; Gale, M., Jr.; Rajagopal, L.; Nelson, B. R.; Ehinger, N.; Mason, B.; Nayeri, U.; Curry, C. L.; Adams Waldorf, K. M. Zika virus and the non-microcephalic fetus: why we should still worry. *Am. J. Obstet. Gynecol.* **2019**, *220* (1), 45−56.
(107) Nguyen, C. T. O.; Hui, F.; Charng, J.; Velaedan, S.; van Koeverden, A. K.; Lim, J. K. H.; He, Z.; Wong, V. H. Y.; Vingrys, A. J.; Bui, B. V.; Ivarsson, M. Retinal biomarkers provide "insight" into cortical pharmacology and disease. *Pharmacol. Ther.* **2017**, *175*, 151−177.
(108) van Wijngaarden, P.; Hadoux, X.; Alwan, M.; Keel, S.; Dirani, M. Emerging ocular biomarkers of Alzheimer disease. *Clin Exp Ophthalmol* **2017**, *45* (1), 54−61.
(109) Dehghani, C.; Frost, S.; Jayasena, R.; Masters, C. L.; Kanagasingam, Y. Ocular Biomarkers of Alzheimer's Disease: The Role of Anterior Eye and Potential Future Directions. *Invest. Ophthalmol. Visual Sci.* **2018**, *59* (8), 3554−3563.
(110) Zhou, L.; Beuerman, R. W. Tear analysis in ocular surface diseases. *Prog. Retinal Eye Res.* **2012**, *31* (6), 527−50.
(111) Wei, Y.; Gadaria-Rathod, N.; Epstein, S.; Asbell, P. Tear cytokine profile as a noninvasive biomarker of inflammation for ocular surface diseases: standard operating procedures. *Invest. Ophthalmol. Visual Sci.* **2013**, *54* (13), 8327−36.
(112) Roy, N. S.; Wei, Y.; Kuklinski, E.; Asbell, P. A. The Growing Need for Validated Biomarkers and Endpoints for Dry Eye Clinical Research. *Invest. Ophthalmol. Visual Sci.* **2017**, *58* (6), BIO1−BIO19.
(113) Schwanhausser, B.; Busse, D.; Li, N.; Dittmar, G.; Schuchhardt, J.; Wolf, J.; Chen, W.; Selbach, M. Global quantification of mammalian gene expression control. *Nature* **2011**, *473* (7347), 337−42.

https://dx.doi.org/10.1021/acs.jproteome.0c00320
J. Proteome Res. 2020, 19, 4496−4515